JIMMA UNIVERSITY
SCHOOL OF GRADUATE STUDIES
JIMMA INSTITUTE OF TECHNOLOGY
FACULTY OF CIVIL AND ENVIRONMENTAL ENGINEERING
HYDROLOGY AND HYDRAULIC ENGINEERING CHAIR
MASTERS OF SCIENCE PROGRAM IN HYDRAULIC ENGINEERING

Evaluation of Climate Change Impact on Stream Flow: A case study of Awash Bello Sub-basin, Upper Awash River Basin, Ethiopia.

By

Abeba Taye

A Thesis Submitted to the School of Graduate Studies of Jimma University, Jimma Institute of Technology in Partial Fulfillment of the Requirements for the Degree of Masters of Science of Technology in Hydraulic Engineering.

APRIL, 2021

JIMMA, ETHIOPIA

JIMMA UNIVERSITY

SCHOOL OF GRADUATE STUDIES

JIMMA INSTITUTE OF TECHNOLOGY

FACULTY OF CIVIL AND ENVIRONMENTAL ENGINEERING

HYDROLOGY AND HYDRAULIC ENGINEERING CHAIR

MASTERS OF SCIENCE PROGRAM IN HYDRAULIC ENGINEERING

Evaluation of Climate Change Impact on Stream Flow: A case study of Awash Bello Sub-basin, Upper Awash River Basin, Ethiopia

By

Abeba Taye

A Thesis Submitted to the School of Graduate Studies of Jimma University, Jimma Institute of Technology in Partial Fulfillment of the Requirements for the Degree of Masters of Science of Technology in Hydraulic Engineering.

ADVISOR: Mr. TOLERA ABDISA (Assist. Prof)

CO-ADVISOR: Mr. BEKAN CHELKABA (MSc)

APRIL, 2021

JIMMA, ETHIOPIA

DECLARATION

I Abeba Taye Worku declare that this thesis entitled: " **Evaluation of Climate Change Impact on Stream Flow: A case study of Awash Bello Sub-basin, Upper Awash River Basin, Ethiopia "** is my original work and that it has not been presented and will not be presented to any other university for similar or any other degree award.

(MSc.) Candidate	Signature	Date
Abeba Taye	--------------------------	----------------------------

We, the undersigned, certify that a dissertation entitled **"Evaluation of Climate Change Impact on Stream Flow: A case study of Awash Bello Sub-basin, Upper Awash River Basin, Ethiopia."** is the original work of Miss**.** Abeba Taye and has been submitted for examination with our approval as university advisors.

Name	signature	Date
Mr. Tolera Abdisa (Assist. Prof)	--------------------------	--------------------------
(Main advisor)		
Mr. Bekan Chelkaba (Msc)	-----------------------------	----------------------------
(Co-Advisor)		

APPROVAL PAGE

This is to certify that the thesis prepared by **Ms. Abeba Taye** entitled **"Evaluation of Climate Change Impact on Stream Flow: A case study of Awash Bello Sub-basin, Upper Awash River Basin, Ethiopia."** and submitted as partial fulfillment for the award of the Degree of Master of Science in Hydraulic Engineering complies with the regulations of the university and meets the acceptance standards concerning originality, content, and quality.

Signed by Examining board:

External Examiner:	Signature	Date
-------------------------------	--------------------------------	--------------------------------
Internal examiner:		
-------------------------------	----------------------------------	----------------------------------
Chairperson:		
-------------------------------	------------------------------------	--------------------------------

ABSTRACT

Climate change impact and its variability on stream flows are now becoming one of the significant challenges. It occurs because of internal variability within the climate system and external factors. The main objective of this study was to evaluate the impacts of climate change on the streamflow of the Awash Bello sub-basin, Ethiopia, using the soil and water assessment tool. This study contributes to putting direction to plan and manage the streamflow sustainability by the water resource sector of the country. For this study Hydrological data, spatial data, and meteorological data were collected from the ministry of water, irrigation, and electricity, the National meteorological service agency respectively, and the regional climate model from the Coordinated Regional Climate Downscaling Experiment Africa was used. Downscaled future climate projections of precipitation and temperature were extracted from Hadley Global Environment Model 2-Earth System) under two radiative forcing scenarios (RCP4.5 and RCP8.5). Before using the input data especially precipitation and temperature to the SWAT, bias correction was made by using power transformation and variance scaling equation for both in line with the observed data, and areal rainfall by Theissen polygon over the sub-basin was determined. The study area was delineated into 35 sub-basins with 218 hydrological response units. The future projection period was divided into two-time horizons the 2050s (2021-2050) as middle-future and 2080s (2051-2080) and as far-future compared with base period (1990–2019). The result obtained shows that projected mean annual precipitation expected to increase by 4.85% in the 2050s and decreased by 9.87% in 2080s under RCP4.5 while under RCP8.5 precipitation increased by 7.56% in 2050s and decreased by 15.21% in 2080s. The projected minimum temperature increased by 0.78^{o}c and 1.12^{o}c for RCP4.5 and 0.93^{o}c and 1.38^{o}c for RCP8.5 in the 2050s and 2080s respectively. Similarly, the maximum temperature increased by 1.06^{o}c and 1.28^{o}c for RCP4.5 and 1.13 ^{o}c and 1.43^{o}c for RCP8.5 in the 2050s and 2080s respectively. The calibration and validation of the model were done using SWAT-CUP and SUFI-2 algorithms and the model indicated good results. The model results showed a good performance with a statistical performance evaluation of R^2 = 0.89, NSE = 0.87 and PBIAS = -11.9 during calibration and R^2 = 0.88, NSE = 0.86 and PBIAS = -17.1 during validation. The mean annual streamflow percentage of changes increased by 4.22% and 5.71% for a period of 2050s under RCP4.5 and RCP8.5 scenarios respectively. While in the 2080's it may decrease by 10.25% and 12.15% under RCP4.5 and RCP8.5 scenarios. Generally, there will be the tendency of variation in streamflow for all future time series. Therefore, it is important to consider this variation of flows to structure appropriate guidelines for planning and management of future and existing water resource projects in this study area.

***Keywords**: Awash Bello, bias correction, Climate Change, CORDEX, SWAT, RCP4.5, RCP8.5*

ACKNOWLEDGEMENT

First of all Praise and thanks to Almighty GOD, the most gracious and the most merciful, for giving me the ability, the health, and the strength to be where I am now. Secondly, I would like to express my sincere thanks and appreciation to my main advisor Mr. Tolera Abdisa, and co-Advisor Mr. Bekan Chelkaba for their thought, advice, and guidance in the preparation of this study.

Next, I extend my deepest gratitude to my sponsor Ethiopian road authority (ERA), and Jimma University for granting me this opportunity to study for a master's science degree. I also thank the National Meteorology Service Agency (NMSA), Ministry of Water, Irrigation and Electricity (MoWIE), for providing me data free of charge.

Last, I would like to express my sincere thanks to the hydrology and hydraulic engineering chair, particularly for staff members for their considerable support in providing me required information, data, and other relevant reference materials, and to my family for their constant encouragement, and moral support without which this thesis would not be done.

TABLE OF CONTENTS

DECLARATION I

APPROVAL PAGE II

ABSTRACT III

ACKNOWLEDGEMENT IV

TABLE OF CONTENTS V

LIST OF TABLES VIII

LIST OF FIGURE IX

ACRONYMS AND ABBREVIATIONS XI

1. INTRODUCTION 1

1.1 Background 1
1.2 Statement of the problem 3
1.3 Objectives 4
1.3.1 General Objective 4
1.3.2. Specific Objectives 4
1.4 Research Question 4
1.5 significance of the study 4
1.6. Scope of Study 5
1.7 Limitation of the study 5

2. LITERATURE REVIEW 6

2.1 Climate Change 6
2.2 Causes of Climate Change 7
2.3 Impacts of Climate Change in Ethiopia 8
2.4 Impacts of Climate Change on Water Resource 10
2.5 Impacts of Climate Change on Streamflow 11
2.6. Climate Models 12

2.6.1 General circulation models (GCM) ... 13
2.6.2 Regional Climate Models (RCMs) ... 13
2.6.2.1 Coordinated Regional Downscaling Experiment (CORDEX) ... 13
2.7. Bias Correction ... 14
2.7.1 Power Transformation for precipitation ... 15
2.7.2 Variance Scaling for Temperature ... 15
2.8 Hydrological Model ... 16
2.8.1. Hydrologic Model Selection Criteria ... 17
2.8.2. SWAT Model and SWAT-CUP ... 18
2.8.2.1 Hydrological components of SWAT ... 19
2.8.2.2 SWAT Calibration and Uncertainties Procedure (SWAT-CUP) ... 20
3. MATERIALS AND METHODS ... 22
3.1 Description of Study Area ... 22
3.2. SWAT Model Description ... 24
3.3 Data collection ... 24
3.3.1 Observed Meteorological Data ... 24
3.3.2 Streamflow Data ... 25
3.3.3 Spatial Data ... 26
3.3.4 CORDEX (RCM) data ... 27
3.4 Data Process and Analysis ... 28
3.4.1 Missing Data Filling ... 28
3.4.2 Data Quality Analysis ... 30
3.4.3 Estimating Areal Precipitation ... 32
3.4.4 RCM data analysis ... 34
3.4.5 Bias Correction ... 35
3.4.5.1. Bias corrected precipitation ... 36

3.4.5.2. Maximum Temperature 37
3.4.5.3 Minimum Temperature 38
3.5 SWAT Model Setup 39
3.5.1 Watershed delineation 39
3.5.2 Hydrologic Response Units (HRU) Definition 40
3.5.3 Weather Generator 42
3.5.4 Weather Data Input Definition 43
3.6 SWAT Model Simulation 43
3.6 SWAT Model Sensitivity Analysis, Calibration, and Validation 44
3.6.1 Sensitivity Analysis 44
3.6.2 Calibration and Validation 45
3.7 SWAT Model Performance Evaluation 45
3.8 Future Climate Change Scenarios 46
4. RESULTS AND DISCUSSIONS 49
4.1 Future projection of climate change 49
4.1.1 Future projection of Climate Impacts on Precipitation 49
4.1.2 Future Projection of Climate Impacts on Minimum Temperature 50
4.1.3 Future Projection of Climate Impacts on Maximum Temperature 51
4.2 Evaluating the performance of the SWAT model 52
4.2.1 Sensitivity Analysis 53
4.2.2 Model calibration and validation 54
4.3. Impact of Future Climate Change on streamflow 56
5. CONCLUSION AND RECOMMENDATION 59
5.1 CONCLUSION 59
5.2 RECOMMENDATION 61
REFERENCE 62
APPENDIX 73

LIST OF TABLES

Table 3-1 Geographic location and meteorological station of Awash Bello sub-basin................ 25
Table 3-2 Selected grid location nearest to the observed station in the study area 35
Table 3-3 Land use land of Awash Bello sub-basin 42
Table 3-4 Soil type of Awash Bello sub-basin 42
Table 4-1 Model efficiencies parameters in calibration and validation periods........................... 55
Table 4-2 Sensitivity ranking of parameters towards water flow 53
Table4-3 Flow sensitive parameters and fitted values.. 54

LIST OF FIGURE

Figure 3.1 Location map of Awash Bello sub-basin.. 23
Figure 3.2: Meteorological station of Awash Bello Sub-basin.. 25
Figure 3.3 Average monthly observed Streamflow of Malka kunture gaging station................. 26
Figure 3.4 Topographical map of Awash Bello sub-basin 27
Figure 3.5 Mean monthly precipitation of stations in Awash Bello sub-basin (1990-2019)........ 29
Figure 3.6 Mean monthly minimum (A) and maximum (B) temperature of stations in Awash Bello sub-basin stations 30
Figure 3.7 Rainfall consistency checking the result of selected meteorological stations............. 31
Figure 3.8 Cumulative deviation and probability of rejecting homogeneity test result of annual Rainfall at Addis Alem gauging station.. 32
Figure 3.9 Theissen polygon of awash Bello sub-basin 33
Figure 3.10 Awash Bello sub-basin selected meteorological stations with RCM grid points and hydrological gauge station locations.. 35
Figure 3.11 Comparisons between mean monthly Precipitation of Observed, bias-corrected RCM, and uncorrected (Raw RCM) of Awash Bello sub-basin stations 37
Figure 3.12 Mean monthly maximum temperatures of bias-corrected, uncorrected, and the observed of stations in Awash Bello sub-basin. 38
Figure 3.13 Mean monthly minimum temperature bias-corrected, uncorrected, and observed of stations of Awash Bello sub-basin.. 39
Figure 3.14 slope of Awash Bello sub-basin 41
Figure 3.15 conceptual framework of the study 48
Figure 4.1 Seasonal and annual precipitations under RCP4.5 and RCP8.5 for 2021-2050 and 2051-2080 50
Figure 4.2 seasonal and annual minimum temperature changes for 2021-2050 and 2051-2080 of RCP4.5 and RCP8.5.. 51
Figure 4.3 seasonal and annual maximum temperature changes for 2021-2050 and 2051-2080 of RCP4.5 and RCP8.5.. 52
Figure 4.4 Hydrograph of the observed and simulated flow from the watershed for the calibration period monthly (2011-2016).. 55

Figure 4.5 Hydrograph of the observed and simulated flow from the watershed for the validation period monthly (2011-2016). 56
Figure 4.6 Scatter diagram for simulated and observed flow during calibration (A) and validation (B) 56
Figure 4.7 annual and seasonal change under RCP4.5 and RCP8.5 for 2021-2050 and 2051-2080 58

ACRONYMS AND ABBREVIATIONS

Arc GIS	Aeronautical Reconnaissance Coverage Geographic Information Systems
AR4	Fourth Assessment report
AR5	Fifth Assessment Report
CMIP5	Coupled Model Inter-comparison Project Phase 5
CORDEX	Coordinated Regional Climate Downscaling Experiment
DEM	Digital elevation method
FAO	Food and Agricultural Organization
GCMs	Global circulation models
GHG	Greenhouse Gases
GIS	Geographic Information System
GLUE	Generalized Likelihood Uncertainty Estimation
HadCM3	Hadley Center for Climate Prediction version 3
HadGEM2-ES	Hadley Global Environment Model 2-Earth System
HRUs	Hydrologic Response Units
IPCC	Intergovernmental Panel on Climate Change
IWMI	International Water Management Institute
LULC	Land Use and Land Cover
m.a.s.l	Meters above sea level
MoWIE	Ministry of Water Irrigation and Electricity
NMSA	National Metrology Service Agency
RCA4	Ross by Centre Regional Atmospheric Climate Model
RCM	Regional climate modeling
RCP	Representative Concentration Pathways
SRES	Special Report on Emission Scenario
SUFI-2	Sequential Uncertainty Fitting Procedure Version 2
SWAT	Soil and Water Assessment Tool
SWAT-CUP	Soil and Water Assessment Tool- Calibration and Uncertainty Programs
UNFCCC	United Nations Framework Convention on Climate Change.

UTM	Universal Transverse Mercator
WCRP	World Climate Research Program
WMO	World Meteorological Organization
WXGEN	Weather Generator

1. INTRODUCTION

1.1 Background

Climate change can be defined as a significant variability or change in climate variables that last for decades or longer (Tadese *et al.*, 2019). It is expressed using averages of the various elements of weather, and also the probabilities of other conditions, including extreme values (Obasi *et al.*, 2018). It is one of the biggest challenges to humanity in the 21st century (Malhi *et al.*, 2021). It includes major changes in temperature, precipitation, and wind patterns among other effects that occur over several decades or longer (Malhi *et al*., 2021. Climate change is expected to aggravate current stresses on water resources variability from population growth, urbanization, and land-use change.

The global climate is always changing, and that can occur for many reasons. To determine the principal causes of observed changes, which must first ascertain an observed climate change is different from other fluctuations that occur without any force at all. Internal variability is the result of processes within the climate system and is the consequence of climate variability without forcing (Group *et al*., 2013).

One of the stressors on water resources is anthropogenic global climate change. Climate factors such as population growth, economic development, urbanization, land-use changes, and natural geomorphic changes all pose a risk to resource sustainability by reducing water supplies or rising demand. In this context, water sector adaptation to climate change will help to improve water quality (Pachauri, 2014).

The impacts of anthropogenic global climate change on the water cycle are already apparent. These impacts include changes in annual river streamflow, shifts in both flood peak magnitude and timing, alterations in flow duration curves, and changes in the magnitude of low-flow periods. Also, changes in natural vegetation cover, land-use practices, crop water requirements, prolonged growing seasons, and soil functions may further alter the hydrological cycle (Hakala, 2020). Climate change has already affected food security due to warming, changing precipitation patterns, and greater frequency of some extreme events (Angelo & Du Plessis, 2017).

One of the potential impacts of climate change will be in the frequency, intensity, and predictability of rainfall. This challenge will eventually influence water availability which will have far-reaching consequences on water supply, agriculture, and hydropower generation among others (Cryosphere *et al.*, 2013). The major effects of climate change are likely to alter the hydrologic cycle and changes in water availability (Shimelash Molla, 2017).

Climate model simulations are necessary for the investigation of the response of the climate system to various forcing, in particular to forcing associated with higher levels of greenhouse gas concentrations. Model simulations include experiments with global and regional climate models, as well as impact models are driven with output from climate models to evaluate the risk related to climate change for natural and human systems (Policymakers, 2018).

According to the IPCC, 2014 report, there will be water stress in tropical Africa, such as Ethiopia (Pachauri, 2014). A recent study in Upper Awash River Basin indicated an increase in streamflow due to an increase in rainfall through the increase in rainfall contradicts the decreasing trend of observed rainfall (Gizaw *et al.*, 2017).

SWAT models are used to predict future and to simulate the effect of climate change on water resources (Tigabu *et al*., 2020). It requires reliable meteorological variables for current and future climate conditions (Teutschbein, 2013). Global climate models (GCMs) provide such information, but their spatial scale is just too coarse for regional impact studies. Thus, GCM output needs to be downscaled to a finer scale through dynamic regional climate models (RCMs) (Gharbia *et al*., 2016). Recently, the Coordinated Regional Climate Downscaling Experiment (CORDEX) which is a dynamic initiative has made multiple RCMs' outputs available for end-users across the African continent (Giorgi & Gutowski, 2015).

This study aims to evaluate the impact of climate change on streamflow of Awash Bello watershed using the SWAT driven by the downscaled future climate projection of CORDEX derived from the CMIP5 climate model under two radiative forcing scenarios of (RCP4.5 and RCP8.5).

1.2 Statement of the problem

Climate change is one of the most important problems affecting the world today, and it is expected to have an impact on hydrological processes. As a consequence, streamflow and groundwater recharge can be influenced. The future impacts of expected climate change on water supplies as a result of global warming triggered by increasing greenhouse gas emissions are addressed (Sci *et al*., 2014a). Climate change-related changes in the hydrological cycle can have a wide range of consequences and risks, and they are influenced by and interact with climatic drivers of change and water management responses. Many of the impacts of climate change are delivered to society by water, agriculture, and transportation sectors (Pachauri, 2014).

Ethiopia is particularly vulnerable to the effects of climate change and has seen some of the worst water shortages in recent decades. As a result, several studies have focused on the possible effect of climate change on the future volume of certain Ethiopian rivers' streamflow (Gizaw *et al.*, 2017). The upper Awash River is the main source of water in the central rift valley, a sub-basin where natural water supplies are becoming increasingly scarce (Gizaw *et al.*, 2017). Climate change poses a major effect on the Awash basin's population and economic productivity. An increasing number of people, advanced irrigation methods, and industrial usages are only a few of the factors that drive up the river demand (Daba & You, 2020). There were a few studies that conducted climate change impact specifically on streamflow for the upper Awash River basin, even less for the awash Bello sub-basin and most studies in the upper awash river basin focuses on flood and sedimentation rather than streamflow (Namara, 2020) (Alemayehu, 2017) (Lemma, 2018).

This study fills the gap mentioned above and contributes to reducing the impact of climate change on Awash Bello streamflow by showing how it appears and affects the streamflow capacity. Different water resource planning and managing sectors encouraged in implementing the solution to reduce this impact over the streamflow through developing environmental protection systems and land use land cover management in the basin for the sustainability of the streamflow.

1.3 Objectives

1.3.1 General Objective

The general objective of the study is to evaluate the impact of climate change on the streamflow of the Awash Bello sub-basin.

1.3.2. Specific Objectives

1. To assess the change in precipitation and temperature for the future period based on RCP4.5 and RCP8.5 climate scenarios.
2. To check the performances of the SWAT model to the simulation of streamflow in the Awash Bello sub-basin
3. To evaluate the impact of climate change on the future streamflow of the awash Bello sub-basin.

1.4 Research Question

1. What are the changes in precipitation and temperature for the future period based on RCP4.5 and RCP8.5 climate scenarios?
2. What are the performances of the SWAT model to the simulation of stream in the Awash Bello sub-basin?
3. What will be the impact of climate change on the streamflow of the Awash Bello sub-basin?

1.5 significance of the study

By investigating the impact of climate change on hydrology, streamflow, and the availability of water, it is possible to increase agricultural productivity, utilize water resources, and properly conserve natural resources. This study helps to mitigate the effect of climate change on streamflow by showing how it manifests and affects streamflow capacity. Different water resource planning and management sectors become encouraged to implement solutions to reduce the impact on streamflow by improving environmental management strategies and land use land cover management in the sub-basin for streamflow sustainability. Also recognizing the current and future climate fluctuations of Awash Bello sub-basin, water resource sectors to develop mitigation measures to keep the stream flowing for many purposes other than water supply for future generations.

1.6. Scope of Study

This study is, essentially a watershed level study with an area extent of 2612km^2 and focuses on performance evaluation of SWAT model, regional climate change impact on the streamflow of the Awash Bello sub-basin. This was achieved by the use of Regional Climate Model (RCM) CORDEX Africa output which was downscaled for future time horizon under RCP 4.5 and RCP8.5 divided two future periods: 2021-2050 as a middle-term and 2051-2080 as a far-term period to generate the future impact of streamflow with baseline period 1990 to 2019 based on IPCC, 2014 most common to use 30 years for climate change assessment.

1.7 Limitation of the study

The land use/cover was assuming it would remain the same at future time horizons. However, in the real world, the land covers change. DEM has downloaded from Alaska Satellite Facility at a website of https://vertex.daac.asf.alaska.edu and CORDEX data (RCM meteorological data) which was downloaded from website https://climate4impact.eu/imactportal/data/esgfsearch.jsp was needed a strong connection which may not be available in this case.

2. LITERATURE REVIEW

2.1 Climate Change

Climate change is a long-term change in the statistical distribution of weather patterns over a period and becoming a major environmental concern because increasing scientific evidence shows the high concentrations of greenhouse gases (GHGs) in the atmosphere, as well as frequent hydro-meteorological extreme events, are becoming a phenomenon of the twenty-first century (Jilo, 2019). Climate change is expected to alter the quantity, quality, and timing of river flow, groundwater recharge, and other hydrological processes (Todd *et al.,* 2020). Climate change leads to significant impacts on life and natural resources. The consequences of global climate change involve opposing impacts on the environment, hydrological cycle, water resources, agriculture and food security, human health, terrestrial ecosystems, and biodiversity.

According to the report of (Pachauri *et al.,* 2007), Climate change is characterized as a statistically significant variation in the climate's mean state or variability over an extended period, usually decades or longer. Therefore, climate change refers to a substantial change within the average weather conditions experienced during a particular region or location. The changes might be seen concerning a significant change in perceived temperature of the region, the amount of rainfall experienced within the region, duration of exposure of the ground to sunlight.

As IPCC, 2013 reported, at the end of the 21st Century, air temperature between 1986- 2005 and 2081-2100 relatively increases from 0.3°C to 1.7°C under RCP 2.6, 1.1°C to 2.6°C under RCP 4.5, 1.4°C to 3.1°C under RCP 6.0 and 2.6°C to 4.8°C under RCP 8.5 over the world (Stocker *et al.,* 2013). Moreover, this report dictates that changes in precipitation will not be uniform. The high latitudes and the equatorial Pacific are likely to experience an increase in average annual precipitation under the RCP 8.5 scenario. In mid-latitude and subtropical dry regions under RCP8.5 average annual precipitation will likely decrease while wet regions under mid-latitude will be increased.

Climate change has the potential to undermine sustainable development, increase poverty, and delay or prevent the realization of the Millennium Development Goals (Pachauri *et al.,* 2007). Climate change has direct and indirect effects on humans, including effects on health and the risk of extreme events affecting lives, livelihoods, and human settlements, as well as impacts on food security and the sustainability of the natural resource-based economic activity (Kangume & Mulungu, 2018).

According to (Policymakers, 2018) special report, Climate change contributes to land stressors, exacerbating existing threats to livelihoods, biodiversity, human and ecosystem health, infrastructure, and food security. In all future GHG emission scenarios, land impacts are likely to worsen. Because of warming, shifting precipitation patterns, and the increased occurrence of certain weather events, climate change has already affected food security.

IPCC (2013) reported that the average air temperature in most parts of Africa has already risen by 0.5°C or more over the last century, and some regions have also seen an increase in heavy precipitation (>95th percentile) events on sub-daily and daily time scales since the early 1950s (IPCC, 2013). Furthermore, according to IPCC (2013), air temperature is predicted to rise by 3°C–6°C across Africa by the late twenty-first century under the Representative Concentration Pathway (RCP8.5) climate scenario, compared to the 1986–2005 baseline, which would have a major effect on Africa's extreme weather (Tariku *et al.*, 2021).

2.2 Causes of Climate Change

Climate change and variability have many significant effects on the hydrological cycle and thus also on hydrology and water resources systems. It may be due to natural internal processes or external forcings such as modulations of the solar cycles, volcanic eruptions, and persistent anthropogenic (man-made) changes in the composition of the atmosphere or land use, and also it could be due to natural climate variability or anthropogenic forcing (e.g., greenhouse gases), or a combination of the two (Pachauri, 2014). Changes in forest cover, such as afforestation, reforestation, and deforestation, have a direct effect on regional surface temperature through water and energy exchanges. Where the forest cover increases in tropical regions cooling results from enhanced evapotranspiration (Policymakers, 2018).

A recent study has attempted at the agricultural sector's high vulnerability to increasing temperatures. Rainfall, maximum and minimum temperatures associated with climate change have been shown to have a direct impact on large crop yields in recent literature (Guntukula, 2019). Human actions such as the burning of fossil fuels and the conversion of land for forestry and agriculture can also lead to climate change (Stocker *et al.*, 2013). These human influences on the climate system have increased significantly since the beginning of the Industrial Revolution. These activities change the land surface and release a variety of substances into the atmosphere, among other things (Canada, 2019) (Agency, 2017). These, in turn, may have an impact on the amount of incoming and outgoing energy, as well as warming and cooling effects on the atmosphere. Carbon dioxide, a greenhouse gas, is the most common by-product of fossil fuel combustion (Agency, 2021).

Ethiopia's vulnerability to climate variability and change arises from a high reliance on rain-fed agriculture, which is extremely vulnerable to climate change, under-development of water supplies, low healthcare coverage, high population growth, low economic development, low adaptive capacity, insufficient road infrastructure in drought-prone areas, and weak institutions, lack of awareness, etc. (NMA, 2007).

2.3 Impacts of Climate Change in Ethiopia

Ethiopia is vulnerable to impacts of climate change given the country has experienced some of the worst drought events in the past several decades. Therefore, many studies have been focusing on the potential impact of climate change on the future streamflow volume of some Ethiopian rivers. The increase in average runoff is associated with the increase in precipitation projection over the catchment. Ethiopia's economy is heavily dependent on rain-fed agriculture that is highly vulnerable to climate change (Deressa, 2011). Regardless of the observed drying trends and recurrent drought since recent years, some of these studies have projected an increase in streamflow of Ethiopian rivers by the mid and late twenty-first century. For example (Dile *et al.*, 2013) suggested that the streamflow of the Gilgel Abay River, which is located in the Lake Tana basin is projected to increase from (2070–2100).

Mekonnen H. Daba suggested in his study on the upper awash basin, the change in rainfall and temperature probably leads to increases in the annual streamflow by 5.79% for RCP4.5 and 7.20% for RCP8.5 in the 2020s, whereas decreases by 10.39% and 11.45% under RCP4.5; and 10.79% and −12.38% for RCP8.5 in the 2050s and 2080s, respectively. Similarly, in the 2020s, an increment of annual runoff was 10.73% for RCP4.5 and 12.08% for RCP8.5. Runoff reduces by 12.03% and 4.12% under RCP4.5; and 12.65% and 5.31% under RCP8.5 in the 2050s and the 2080s, respectively (M. H. Daba & You, 2020), (Setegn *et al.* 2011) suggested that the streamflow of the Lake Tana basin, which is the source of the Blue Nile, is mostly projected to decline for 2080–2100. For the whole Nile basin, for which Ethiopia contributes the majority of its annual runoff. Other Ethiopian river basins, such as the Awash basin, (Hailemariam, 1999) simulated a decrease in its streamflow under the impact of climate change in the twenty-first century. Climatic Change as yet, most studies that investigated the potential impact of climate change on water resources of Ethiopia are based on SRES climate scenarios of (Reay *et al.*, 2007) and with a primary focus on the Abay (Blue Nile) basin. Tebikachew suggests that upper blue Nile is possible to experience more frequent and severe hydrologic extremes (flooding and droughts) in the future (Tariku *et al.*, 2021).

Therefore, the key objective of this study is to evaluate the possible impact of climate change on streamflow of Awash Bello catchment, upper Awash River basin using RCP (Representative Concentration Pathways) climate projections (RCP4.5 and RCP8.5). The results of this study should contribute to the long-term water resources planning and adaptation strategies for the Ethiopian region.

The Trend analysis of annual precipitation in Ethiopia shows that precipitation remained more or less constant when averaged over the whole country while a declining trend has been observed over the Northern and Southwestern and the spatial variation of precipitation was influenced by the changes in intensity, position, and movement of direction rain-producing systems over the country (Reay *et al.*, 2007). According to NMA (2007) discovered that in Ethiopia climate variability and change in the country are mainly established through the variability and a decreasing trend in precipitation and increasing trend in temperature (NMA, 2007).

Related to rainfall and temperature change and variability, there were recurrent drought and flood events in the country. There was also observation of water level rise and dry up of lakes in some parts of the country depending on the general trend of the temperature and rainfall pattern of the regions (Mammo, 2017).

The SWAT model application was calibrated and validated in some parts of Ethiopia. A study conducted on modeling of the Lake Tana basin with SWAT model also showed that the SWAT model was successfully calibrated and validated (Setegn *et al.*, 2011). This study reports that the model can produce reliable estimates of streamflow and sediment yield from complex watersheds. (Yimer, 2018) used it to evaluate the climate change impact on streamflow of mill watersheds.

According to this study, the catchment streamflow will have significant changes under predicted changes in precipitation and temperature and indicates that the SWAT model simulates the runoff considerably well for the study area. (Shimelash Molla, 2017) used it to assess the Climate Change Impact on streamflow of Baro Catchment. This study recognized the high vulnerability of streamflow to changes in temperature and rainfall in the catchment. (Werke, Z. 2016) used the SWAT model to predict streamflow and sediment yield modeling of Anger watershed. According to this study, the SWAT model performed well in predicting sediment yield to the Anger River. The study further put that the model proved to be worthwhile in capturing the process of streamflow and sediment transport of the Anger River. (Weregna, 2019) also used to model the Rainfall-Runoff of Dabus River Watershed.

2.4 Impacts of Climate Change on Water Resource

Climate change affects regional hydrologic patterns, which has a variety of consequences for water resource systems. The effects of such hydrologic changes can be experienced in almost every aspect of human life. Climate change is expected to influence the spatial and temporal distribution of water resources due to changes in temperature and precipitation patterns (Sci *et al.,* 2014a).

Climate change has also the potential to decline the surface water quality due to increased evapotranspiration, lower flows, and rivers becoming warmer, making the management of water treatment works. The decrease in runoff volume would result in a reduction in the water supply. Temperature increases, changes in precipitation patterns and snow cover, and a potential rise in the frequency of floods and droughts are the major global climate change effects associated with water supplies.

Many types of research are finding the impact of climate change on water resources. For example (Bekele *et al.,* 2019), on their finding, over the coming decades, increased rainfall, warmer temperatures, and a significant increase in the hydrologic components, particularly excess runoff and associated extreme peak flow over keleta watershed in the Awash River Basin, (Tay*e et al.,* 2018) also predict that decrease in water availability over time indicates increased water stress in the basin, as well as a risk of water protection for various sectors over the awash basin, (Sci *et al.*, 2014b), suggested that there is also high confidence in the projection that many semi-arid areas will suffer a reduction in water resources due to climate change, (Legesse Gebre, 2015) also found that the projected increase of runoff associated with the increase in precipitation over the catchment at 2030`s and 2090`s future periods, According to (Abbasa *et al.,* 2016) predicted that the whole basin will be extremely dry in near (2046-2064) and far future (2080-2100) which showed a worsening water resources regime into the future in Iraq. (Desta, 2017) suggest that the Gibe III basin is likely to face more floods in both future periods while low flows are projected to decrease.

2.5 Impacts of Climate Change on Streamflow

Streamflow is the amount of water flowing in a river and it is always changing every time. It is mainly influenced by precipitation runoff in the watershed that causes rivers to rise. Increasing temperature, temporal and spatial variability of rainfall distribution are a significant challenge in the variability of streamflow in the Awash Bello sub-basin, and these changes of climate variables in the area severe direct impact. The main influence on streamflow is precipitation runoff fluctuation in the watershed. Rainfall causes rivers to rise, and a river can even rise if it only rains very far up within the watershed. Recall that water that falls in a watershed will eventually drain by the outflow point. The level of streamflow will be affected by several factors which include rainfall characteristics, soil physical properties, watershed factors, and human activities (Tadese *et al.,* 2019).

The change in global temperature always shows an increasing trend and increases in sea level as a result of melting ice for the past time frame. If these changes are continuing in these patterns climate change might have an appalling impact on natural resources and human beings. There is very high confidence, based on more evidence from a wider range of studies, that recent warming is strongly affecting hydrology, ecosystem, and freshwater availability (Doktor-ingenieur *et al.,* 2013).

In recent decades, climate change has become a major concern due to emissions of greenhouse gases and other trace gases in the atmosphere (Pachauri, 2014). Changes in hydrologic cycles and water availability are likely to be one of the most important consequences of climate change.

Increased evaporation, combined with changes in precipitation, has the potential to affect runoff, Streamflow (encompasses surface flow, subsurface flow, and groundwater flow), the frequency and intensity of flood and drought frequency and severity, soil moisture, and water availability for irrigation and hydroelectric generation (Bokke *et al.*, 2017).

Many studies have been focusing on the impact of climate change on streamflow. For instance, the study of (Roth *et al.*, 2018) shows that the rainfall is expected to be strong undercurrent climate scenarios in the main rainy season that has a direct consequence on streamflow of the Blue Nile basin, (M. H. Daba & You, 2020) predict that, streamflow in upper awash river basin is expected to decrease in 2050s and 2080s, (Yimer, 2018) suggested that the streamflow of Mille catchment, which is located in the lower-Awash basin will have significant changes under predicted changes in precipitation and temperature, (Demissie *et al.*, 2013) for the Gilgel Gibe 1 project which is located in the south-western part of Ethiopia, in the Oromia Regional State, the simulation indicates a decrease in predicted streamflow and an increase in predicted sediment flux for the future period of the 2050s, (Setegn *et al.*, 2011) suggested that the streamflow of Lake Tana basin, which is the source of the Blue Nile, is mostly projected to decline for 2080–2100, For other Ethiopian river basins, such as the Awash basin, (Hailemariam, 1999) simulated a decrease in its streamflow under the impact of climate change in the twenty-first century.

2.6. Climate Models

Model is a physical, mathematical, or otherwise logical representation of a system, entity, phenomenon, or process and representation of one or more concepts that may be realized in the physical world.

Climate models are a very complex system, with many components and remarkable tools for understanding the complexity of our Earth’s climate system. According to IPCC (2013), climate models have continued to be developed and improved. To simulate the climate system, these models use a series of equations (derived from physical, chemical, and biological laws). They can simulate the past or future states of a climate system over periods ranging from a few hours to centuries. These simulations can supplement observed climate data from a sparse global observation network, i.e. reanalysis (Abiodun & Adedoyin, 2016).

2.6.1 General circulation models (GCM)

General circulation models, or GCMs, are climate models that use mathematical equations to define how energy and matter interact in various parts of the ocean, atmosphere, and land. Identifying and quantifying Earth system processes, describing them with mathematical equations, setting variables to represent initial conditions and subsequent changes in climate forcing, and repeatedly solving the equations using powerful supercomputers are all part of the process of building and running a climate model (Steve, 2020).

Global climate models (GCMs) and Regional climate model (RCMs) data are required to project and quantify the relative change of climate variables between current and future periods. GCMs are simulating large-scale mass and energy exchange mechanisms across the globe, by solving three-dimensional governing equations for the atmosphere, ocean, and land surface. Moreover, it is a numerical model that applies physical, chemical, and biological principles to simulate the interaction of the atmosphere, oceans, land surface, snow, ice, and permafrost in determining the earth's climate. However, the outputs are not interpreted as absolute or deterministic predictions of future conditions on specific dates; rather, the GCMs were run multiple times with slightly different initial conditions (Elbehri, 2015).

2.6.2 Regional Climate Models (RCMs)

Regional Climate Models (RCMs) are conceptually similar to GCMs. However, it focuses on specific regions and is driven by GCMs over a limited area, and can provide information at a fine resolution comparable to GCMs (IPCC, 2013). Coarser resolution of climate datasets represented by GCM while the finer resolution of climate data sets represented by RCMs provides a more accurate and detailed representation of localized extreme events (Todd *et al.*, 2020). Thus, RCMs are widely used worldwide for climate change impact assessment particularly for agriculture, hydrology, water resources, and others.

2.6.2.1 Coordinated Regional Downscaling Experiment (CORDEX)

CORDEX is an internationally coordinated effort to support climate change impact and adaptation studies by making relatively fine-scale (approximately 50km×50km) climate projections readily available to users. Downscaling is through an RCM by using initial conditions and boundary conditions as obtained from selected eight GCMs or from reanalysis data which is a merged climate model and observed data (https://cordex.org). The numerical boundary conditions for RCM simulations can, for instance, include vertical profiles of climate variables and surface conditions over oceans. In principle, RCMs cannot remove GCM biases related to large-scale variables (Haile & Rientjes, 2015). Africa was selected as the first target region. CORDEX-Africa RCMs generate an ensemble of high resolution historical and future climate projections at a regional scale by downscaling different GCMs forced by RCPs based on the Coupled Intercomparison Project Phase 5 (CMIP5) (Taylor *et al*., 2012)

CORDEX-Africa tries to fill the gap systematically. The CORDEX data will be calculated using Regional Climate Models (RCM) together with a technique called dynamical downscaling (https://cordex.org). The inter-combination of CORDEX and RCM in assessing and projecting climate change will be used in detail to evaluate the impact of climate change on the Awash Bello watershed. In this study, climate change scenarios data from the newly available CMIP5, RCM output of CORDEX-Africa for African domain projections under Representative Concentration Pathways (RCP4.5 and RCP8.5) were used as input to the hydrological model. CORDEX-Africa prioritizes the RCP4.5 and RCP8.5 scenarios following the priority by CMIP5 (Haile & Rientjes, 2015).

2.7. Bias Correction

Bias correction is an adjustment of modeled values to reflect the observed distribution and statistics. It is required because the downscaled output of climate data stored could not be used directly for impact studies in case of significant biases like precipitation and Temperature can be too high, Model does an incorrect simulation of the monsoon, the rains start too early or too late and Climate models tend to overestimate the number of days with rain and underestimate precipitation extremes (Dierickx, 2019). Bias correction is usually needed because of systematic model errors caused by imperfect conceptualization, discretization, and spatial averaging within grid cells, climate models often provide biased representations of observed time series (Kefeni *et al.,* 2020). Therefore Bias correction is applied in climate impact studies to correct the climate input data provided by regional climate models for systematic statistical deviations from observation data. It is applied to compensate for any tendency to overestimate or underestimate the mean of downscaled variables.

There are different types of bias correction methods for precipitation and temperature. In this study, Power Transformation for precipitation and Variance Scaling for Temperature are used.

2.7.1 Power Transformation for precipitation

The precipitation is usually varied spatially and highly nonlinear. Power transformation is a nonlinear method that corrects both mean and variance of precipitation (Yang, *et al*, 2015). In this study, the RCM data of precipitation was bias-corrected by using the Power Transformation Method because it corrects the mean, variance, and coefficient of variation (CV), which leads to a better copy of observed precipitation. The correction method is applied by comparing the daily observed precipitation at each station with the nearest grid point of the RCM considering the grid points as a single station on the watershed. The power transformation method is explained in equation 2.1.

$$P^* = a.P^b \quad \text{...} \quad 2.1$$

Where P* is corrected precipitation, P is simulated precipitation. The parameters a and b is estimated by equalizing the coefficient of variation (CV) of the corrected simulations P^b and CV of the observed values, both from the calibration/optimization period. Parameter b was first determined iteratively by ensuring that the CV of the corrected precipitation matched that of the observed. Then parameter a, which depends on the value of b, was determined by matching the means of the corrected and observed precipitation (Terink *et al.*, 2010). In this way, the CV is only a function of parameter b according to:

$$CV\ (P) = f\ (b)$$

2.7.2 Variance Scaling for Temperature

The Power transformation method is an effective method to correct both the mean and variance of precipitation, but it cannot be used to correct temperature time series, as the temperature is known to be approximately normally distributed (Yang *et al,* 2015). The VARI method was developed to correct both the mean and variance of normally distributed variables such as temperature (Teutschbein and Seibert, 2012). Temperature is normally corrected using the VARI method with the equation 2.2.

$$T_{corr} = \overline{T}_{\text{obs}} + \frac{\sigma(T_{obs})}{\sigma(T_{rcm})} (T_{rcm} - \overline{T}_{rcm}) \quad \text{……………………………………………2.2}$$

Where T_{Corr}: the corrected daily temperature. T_{rcm}: the uncorrected daily temperature from RCM model and T_{obs}: the observed daily temperature while $\overline{T}_{obs}$ is the mean observed temperature and $\overline{T}_{rcm}$ is the mean simulated temperature.

2.8 Hydrological Model

Hydrological models are mathematical descriptions of elements of the hydrologic cycle. They have been developed for several different reasons and thus have many different forms. However, hydrological models are in general designed to meet one of the two primary objectives. The one objective of the watershed hydrologic modeling is to get a better understanding of the hydrologic processes in a watershed and of how changes in the watershed may affect these phenomena (Lenhart, *et al*, 2002). Based on process description, the hydrological models can be classified into three main categories (Cunderlik, 2003)

Lumped models Parameters of lumped hydrologic models don't vary spatially within the basin and thus, basin response is evaluated only at the outlet, without explicitly accounting for the response of individual sub-basins. The parameters often don't represent physical features of hydrologic processes and usually involve a certain degree of empiricism (Geremew, 2013). These models are not usually applicable to event-scale processes. If the interest is primarily in the discharge prediction only, then these models can provide just as good simulations as complex physically-based models (Gebre, 2015).

Distributed models Parameters of distributed models are fully allowed to vary in space at a resolution usually chosen by the user. Distributed modeling approach attempts to include data concerning the spatial distribution of parameter variations among computational algorithms to evaluate the influence of this distribution on simulated precipitation-runoff behavior (Mohammed, 2013). Distributed models usually require a large amount of (often unavailable) data. However, the governing physical processes are modeled in detail, and if properly applied, they can provide the highest degree of accuracy (Akpoti, 2016a).

Semi-distributed models Parameters of semi-distributed (simplified distributed) models are partially allowed to vary in space by dividing the basin into several smaller sub-basins (Chandra *et al*., 2019). The main advantage of these models is that their structure is more physically based than the structure of lumped models, and they are less demanding on input data than fully distributed models (Arnold *et al*., 2010). SWATS, HEC-HMS, are considered semi-distributed models. Hydrologic models can be further divided into event-driven models, continuous process models, or models capable of simulating both short-term and continuous events (Leta, 2017). Event-driven models are designed to simulate individual precipitation-runoff events. Their emphasis is placed on infiltration and surface runoff. Typically, event models haven't any provision for moisture recovery between storm events and, therefore, aren't fitted to the simulation of dry-weather flows. Instead, continuous-process models simulate an extended period, predicting watershed response both during and between precipitation events. They are suited for simulation of daily, monthly or seasonal streamflow, usually for long-term runoff volume forecasting and for estimate of water yield (Cunderlik,2003).

2.8.1. Hydrologic Model Selection Criteria

The selection of hydrological models is based on various criteria that can be used for choosing the right hydrological model for a specific problem. These criteria are always project-dependent since every project has its specific requirements and needs. The criterion used to select the SWAT model is based on the benefits it's providing to the objectives of the study. Further, some criteria also are user-depended (subjective). Among the various project-dependent selection criteria, there are four common, fundamental ones that must be always answered (Geremew, 2013);

- Required model outputs important to the project and therefore to be estimated by the model (Does the model predict the variables required by the project such as a long-term sequence of flow and sediment yield?)
- Hydrologic processes that need to be modeled to estimate the desired outputs adequately (Is the model capable of simulating single-event or continuous processes?)
- Availability of input data (Can all the inputs required by the model be provided within the time and cost constraints of the project?)
- Price (Does the investment appear to be worthwhile for the objectives of the project?)

Reasons for the selecting SWAT model was its best application for land use and land cover change and climate change impact assessment in different parts of the world and simulates the major hydrological process in the watersheds as well as it is less demanding on input data plus it's readily and freely available.

2.8.2. SWAT Model and SWAT-CUP

The SWAT model is a semi-distributed physically-based simulation model and can forecast the impacts of land-use change and management practices on hydrological regimes in watersheds with varying soils, land use, and management conditions over long periods and primarily as a strategic planning tool (Akpoti *et al*., 2016). SWAT is one of the most widely used watersheds modeling tools, applied extensively in a broad range of water quantity and quality problems worldwide and it can predict the effects of soil, land use, and management on water. The SWAT model requires intensive data including topography, soil, land use, and weather data as input (Sab-basin & Daba, 2018).

The interface of the SWAT model is compatible with ArcGIS that can integrate numerous available geospatial data to accurately represent the characteristics of the watershed. In the SWAT model, the impacts of spatial heterogeneity in topography, land use, soil, and other watershed characteristics on hydrology are described in subdivisions (Geremew, 2013). There are two scale levels of subdivisions; the first one is that the watershed is divided into several sub-watersheds based upon drainage areas of the attributes, and the other one is that each sub-watershed is further divided into several Hydrologic Response Units (HRUs) based on land use and land cover, soil and slope characteristics.

Streamflow is determined by its components (surface runoff and the groundwater flow from shallow aquifers). To capture the spatial and temporal variations of the watershed, it is necessary to delineate the watershed into smaller-sized sub-basin areas where the variables can be considered homogenous. Furthermore, the digital elevation model (DEM) was used to divide the watershed into several hydrological response units and to predict the location of the stream. The land use and soil maps were used to define the characteristics of land cover and soil properties of the watershed, respectively. Using the combination of the land use, DEM, soil, and slopes, the hydrological response units were developed to simulate the basin characteristics. Furthermore, a weather generator model from statistical data summarized over long-term monthly average series was developed to fill missing values and to generate the other climatic parameters (wind speed, sunshine hours, and solar radiation) (Geremew, 2013).

2.8.2.1 Hydrological components of SWAT

The SWAT model simulates eight major components: hydrology, weather, sedimentation, soil temperature, crop growth, nutrients, pesticides, and agricultural management. Major hydrologic processes that can be simulated by this model include evapotranspiration, surface runoff, infiltration, percolation, shallow aquifer, and deep aquifer flow, and channel routing (Arnold *et al.*, 2010).

SWAT simulations consist of two main parts: a land phase and a routing phase. During the land phase, the daily loadings of water and pollutants are calculated for each sub-basin. In the second phase, which is the routing phase, these loadings are routed via the main channel network to the outlet of the basin (Cambien *et al*., 2020). The hydrological components in the model are based on the water balance equation given in equation (2.3) below (Dibaba *et al*., 2020). Water balance is the driving force behind everything that happens in the watershed (Akpoti *et al*., 2016) (Leng *et al*., 2020).

$$SW_t = SW_o + \sum_{i=1}^{t}(R_{day} - Q_{\mathrm{surf}} - E_a - W_{seep} - Q_{gw}) \quad \text{......................2.3}$$

where SW_t is the final soil water content (mm), SWo is the initial water content (mm), t is the time (days), R_{day} is the amount of precipitation on the day i (mm), $Q_{\mathrm{surf}}$is the amount of surface runoff on a day i (mm), E_a is the amount of evapotranspiration on the day i (mm), Wseep is the amount of water entering the vadose zone from the soil profile on the day i (mm) and Q_{gw} is the amount of return flow on the day i (mm).

Surface Runoff

To predict the surface runoff curve number method is used. Therefore, the SWAT model uses the Soil Conservation Service (SCS) curve number method and the Green and Ampt infiltration methods to simulate surface runoff volume and peak rates for each HRU (Cambien *et al*., 2020) (Akpoti *et al*., 2016). The curve number equation is given as:

$$Q_{surf} = \frac{(R_{day} - I_a)^2}{(R_{day} - I_a + S)} \quad \ldots\ldots 2.4$$

Where Q_{surf} is the accumulated runoff or rainfall excess (mm); R_{day} is the height of rainfall for the day (mm); Ia is the initial abstractions (canopy interception, surface storage, infiltration before runoff) (mm), and S the retention parameter. Therefore, retention parameter S is defined as Equation (2.5):

$$S = 25.4\left(\frac{1000}{CN}\right) - 10) \quad \ldots\ldots 2.5$$

Where CN is the curve number for the day and the initial abstractions, Ia, are commonly approached as 0.2S. Equation (2.6) is denoted as follows:

$$Q_{surf} = \frac{(R_{day} - 0.2S)^2}{(R_{day} + 0.8S)} \quad \ldots\ldots 2.6$$

The runoff will only occur when R_{day} > Ia

2.8.2.2 SWAT Calibration and Uncertainties Procedure (SWAT-CUP)

SWAT-CUP is an interface that was developed for SWAT. Using this generic interface, any calibration/uncertainty or sensitivity program can easily be linked to SWAT (Abbaspour *et al.*, 2015). The SWAT-CUP program is linked to four algorithms to run calibration and validation in SWAT models. These include

I. Generalized Likelihood Uncertainty Estimation (GLUE)
II. The Sequential Uncertainty Fitting (SUFI-2) method
III. The Parameter Solution and
IV. The Bayesian inference is based on the Markov Chain Monte Carlo (MCMC) method.

SUFI-2 algorithm, in particular, is suitable for calibration and validation of SWAT models because it represents uncertainties of all sources (e.g., data, model) (Yang *et al.*, 2008). It can perform parameter sensitivity analysis to identify those parameters that contributed the most to the output variance due to input comprehensive description on the SUFI-2 algorithm.

2.8.4.1 Calibration and Validation

The first step of model calibration and validation is sensitivity analysis. Its primary objective is to identify parameters that have a great influence on model outputs (e.g., streamflow). The global sensitivity analysis method used to determine sensitive parameters, using the SUFI-2 method of SWAT-CUP Global sensitivity analysis distinguishes the sensitive rank of whole considered parameters related to streamflow by Latin hypercube regression analysis (Abbaspour, 2015).

The sensitivity of parameters depends on the t-stat and p-value; two statistical measurements could assess the sensitive rank of each parameter. The t-state represents a range of sensitivity, while the p-value identifies the significance of sensitivity. The higher absolute value of t-stat and lower value of p-value is the most sensitive parameter (Thavhana *et al*., 2018).

Calibration in a hydrological model is the process of estimating model parameters by comparing the model prediction with the observed data for the same condition. Calibrations are very important for parameters that were not measured and are essentially heterogeneous and uncertain, as it serves to optimize the unknown model parameters (Dibaba *et al*., 2020). Validation is used for the comparison of the model results with an independent dataset during calibration without any further adjustment of the calibration parameters.

3. MATERIALS AND METHODS

3.1 Description of Study Area

The Awash River Basin is one of the twelve major river basins of Ethiopia and the fourth largest basin in Ethiopia and originates around Ginchi Town west of Addis Ababa and ends at Lake Abe, flowing 1,250 km through different regions of Ethiopia. It rises in the central high plateau of altitude 3000 meters above sea level (a.m.s.l) (Todd *et al.*, 2020). Unlike many Trans boundary Ethiopian Rivers, the Awash River rises and terminates in the country. The total area of the Awash River Basin covers is 112,000 km^2, and the water resource in the basin is estimated to be 4.9 billion cubic meters (BM^3) of annual flow (Namara, 2020).

Awash Bello sub-basin is located along the Awash River in the upper part of the Awash River basin with a total catchment area of 2612 km^2. It is one of the flood plains of the basin that faced frequent flood damage due to the overflow of the Awash River Basin, Ethiopia. It is located to the southwest of the basin in the upper part near the source of Awash River between 8^0 35’0’’ to 9^0 30’0’’ N latitude and 38^0 0’0” to 38^0 38’0’’E longitudes on a geographical basis at a distance of 55km from Addis Ababa (Namara, 2020).

The climate of the awash Bello sub-basin is categorized as humid to sub-humid with a mean monthly precipitation of sub-basins varies from 938.71mm to 1548.92mm based on the variation in elevation and the mean monthly minimum and maximum temperature of the stations ranges from 9.67°C to 11.29°C and 23.8°C to 27.13°C respectively. Malka Kunture River is one of the major rivers which contribute a significant amount of flow to the Awash River. The flow of the Malka Kunture River is strongly seasonal. The mean monthly flow is up to 168.91m3/s. Peak flows usually occur in August. Awash Bello sub-basin has different land use/cover and about 87% of the land is dominated by intensively cultivated land and followed by moderately cultivated land. It also consists of different soil types among which pellic vertisols cover more than 80% of the area.

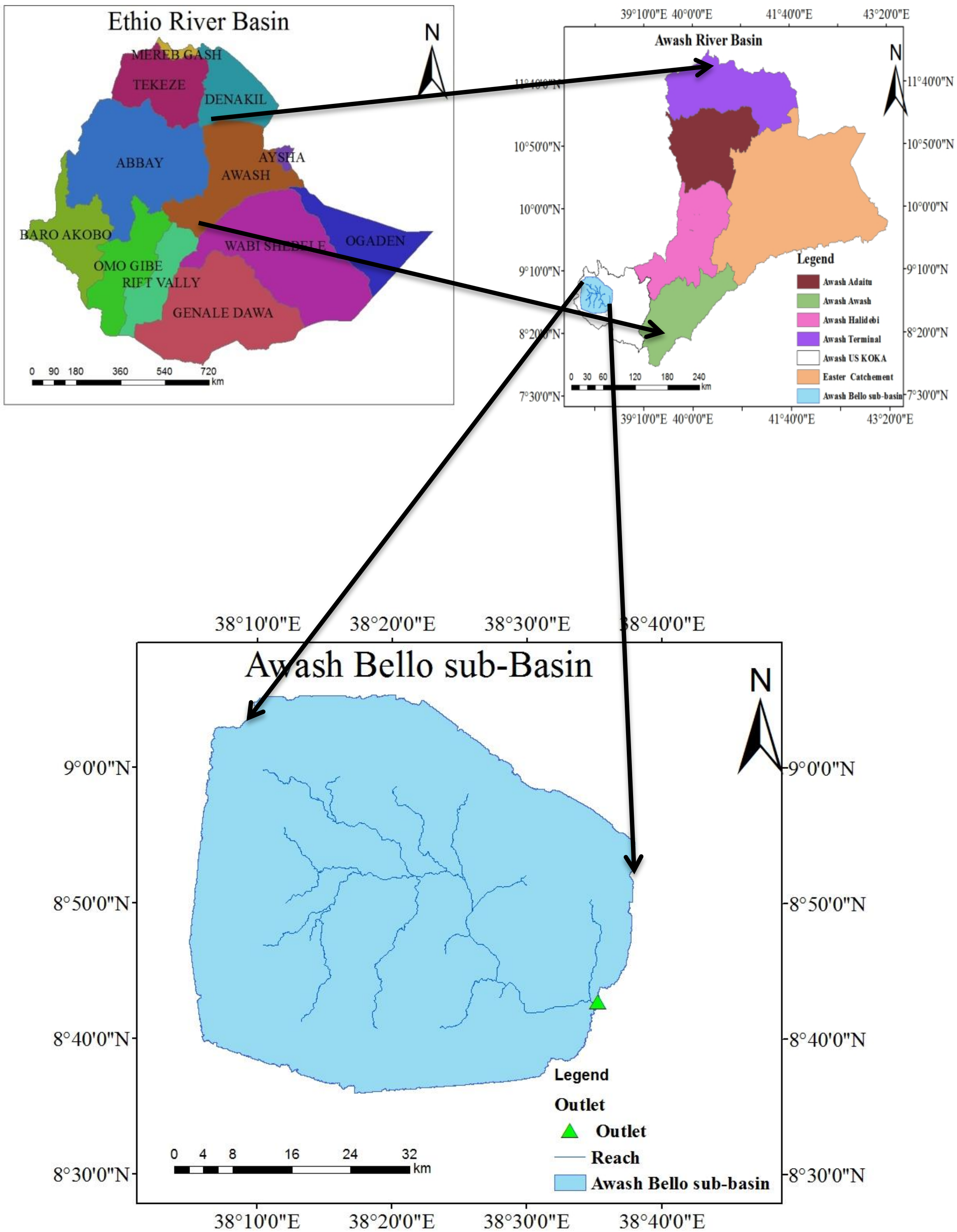

Figure 3.1 Location map of Awash Bello sub-basin

3.2. SWAT Model Description

Soil and Water Assessment Tool (SWAT) is a model designed on continuous-time and spatially distributed for the simulation of water, sediment, and nutrient and pesticide transport at a catchment scale on a daily time step (Aawar & Khare, 2020). It is used to predict the influence of land use and land cover change on water in a vast watershed over a long time with different conditions (Gashaw *et al*., 2018). The model calculations are performed on an HRU basis and flow and water quality variables are routed from HRU to sub-basin and subsequently to the watershed outlet. The SWAT model simulates hydrology as a two-component system, comprising land hydrology and channel hydrology (Gebrie *et al*., 2016). Water balance is the driving force behind everything that happens in the watershed (Akpoti *et al*., 2016) (Leng *et al*., 2020).

$$SW_t = SW_o + \sum_{i=1}^{t}(R_{day} - Q_{\mathrm{surf}} - E_a - W_{seep} - Q_{gw}) \quad \text{....................[3.1]}$$

where SW_t is the final soil water content (mm), SWo is the initial water content (mm), t is the time (days), R_{day} is the amount of precipitation on the day i (mm), $Q_{\mathrm{surf}}$is the amount of surface runoff on a day i (mm), E_a is the amount of evapotranspiration on the day i (mm), Wseep is the amount of water entering the vadose zone from the soil profile on the day i (mm) and Q_{gw} is the amount of return flow on the day i (mm).

3.3 Data collection

3.3.1 Observed Meteorological Data

Meteorological data is required as input to the SWAT model in hydrological model development. For this study, daily data of precipitation, temperature (Max & Min), sunshine hour, relative humidity, and wind speed of five stations in the Awash Bello watershed, were collected from the National Meteorological Service Agency (NMSA). The length of data collected from station to station was uniform as it was recorded from the year 1990 to 2019.

Table 3-1 Geographic location and meteorological station of Awash Bello sub-basin

STATION	LAT	LONG	ELEVATION (m)
Addis alem	9.042	38.382	2372
Ginchi	9.02	38.133	2132
Tulu bolo	8.67	38.22	2100
Tefki	8.84	38.489	2063
Teji	8.833	38.367	2091

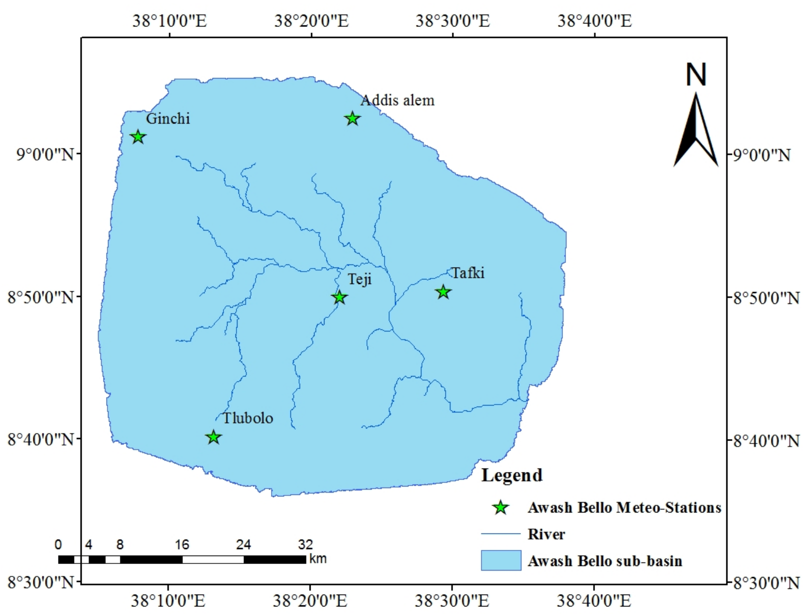

Figure 3.2: Meteorological station of Awash Bello Sub-basin

3.3.2 Streamflow Data

Hydrological data is one more essential input data required for simulating streamflow in modeling. The main function of this data is for performing sensitivity analysis, calibration and Uncertainty analysis, and validation of the model. The hydrological data used in this study were collected from the Ethiopian Ministry of water, irrigation, and electricity (MoWIE) department of Hydrology for the Melka Kunture's streamflow gauging station which is found at the outlet of the Awash Bello sub-basin. The observation period of the collected data covers from 2000 to 2016 which are daily time series data.

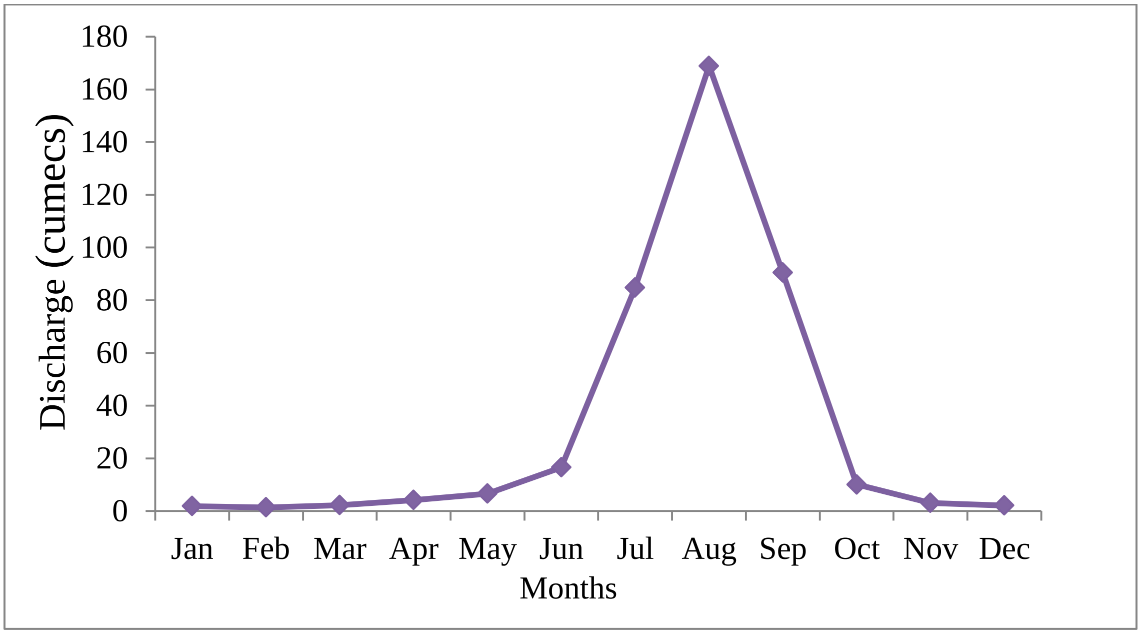

Figure 3.3 Average monthly observed Streamflow of Malka kunture gaging station

3.3.3 Spatial Data

1. Digital Elevation Model (DEM) Data

Digital elevation model that was used for extraction of watershed characteristics such as Drainage area, stream network, flow direction, flow accumulation, slope, elevation, sub-basin, and as general for study area delineation was downloaded from ALASKA SATELLITE FACILITY at a website of https://vertex.daac.asf.alaska.edu. It was a recently uploaded topographic feature with a high resolution of 12.5mx12.5m cell size and spatial reference of WGS_84_UTM_ZONE_37N. This topographic data or digital elevation is found between elevation ranges of 1988m to 2887m (a.m.s.l).

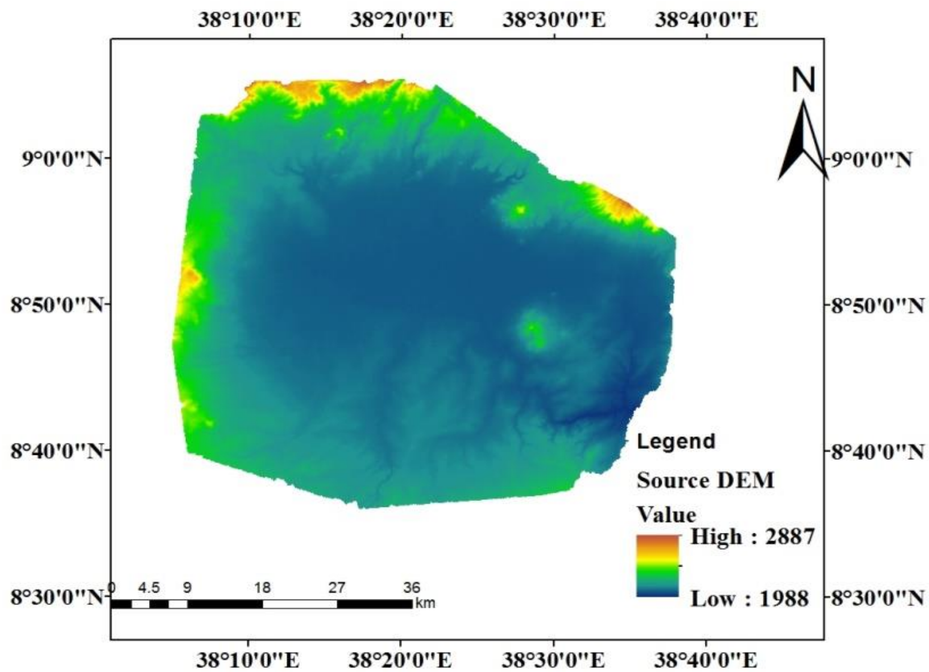

Figure 3.4 Topographical map of Awash Bello sub-basin

2. Land use / Cover Data

Land use/cover data in a watershed are one of the influential factors which affect surface runoff, evapotranspiration, and erosion and used to simulate the growth of a particular land cover. The Land use/cover data as shapefiles were obtained from the Ministry of Water, Irrigation, and Electricity (MoWIE), department of Geographic Information System (GIS).

3. Soil Data

Soil data is one of the major input data for the SWAT model. Different soils have different properties, which affect the surface runoff, sediment yield, and water balance of the sub-basin. The soil map of the study area as a shapefile, the Food and Agricultural Organization (FAO) digital soil database, collected from the Ethiopian Ministry of Water, Irrigation and Electricity, Department of Geographic Information System was used.

3.3.4 CORDEX (RCM) data

Regional Downscaled climate data have been obtained from the CORDEX-Africa database. It is available at a spatial resolution of 0.44° by 0.44° (approximately 50km). International water management institute (IWMI) provided the predicted future climate change parameters of rainfall and temperature data on grid point-based. The future climate simulation was conducted to determine the impact of two specific scenarios of RCP4.5 and RCP8.5 in the catchment. For this study, precipitation and maximum and minimum temperature datasets are downloaded from the CORDEX-Africa website (https://climate4impact.eu/impactportal/data/esgfsearch.jsp).

3.4 Data Process and Analysis

Data Processing is a series of actions or steps performed on data to verify, organize, transform, integrate, and extract data in an appropriate output form for subsequent use. Methods of processing must be thoroughly recognized to ensure the utility and integrity of the data. Data analysis involves actions and methods performed on data that help describe facts, detect patterns, develop explanations, and test hypotheses. Before beginning any hydrological analysis, it is important to make sure that data are homogenous, consistent, sufficient, and complete with no missing values. Errors resulting from lack of appropriate data processing are serious because they lead to bias in the final results (Vedula & Mujumdar, 2005).

3.4.1 Missing Data Filling

3.4.1.1 Precipitation Data

Due to any rain gauge or the absence of observer or instrument failure, meteorological data records occasionally are incomplete. The gaps should be estimated first before we use the rainfall data for any analysis. The nearby stations located within the catchment help to fill the missing data on the assumption of hydr o-meteorological similarity of the group of stations. In this study, the Stations with missing data were filled by multiple imputation using XLSTAT2015 by filling each from its neighboring stations. Having filled the entire precipitation data gap, average monthly precipitation of the Awash Bello sub-basin was shown in (figure 3.5) during the dry season and rainy season.

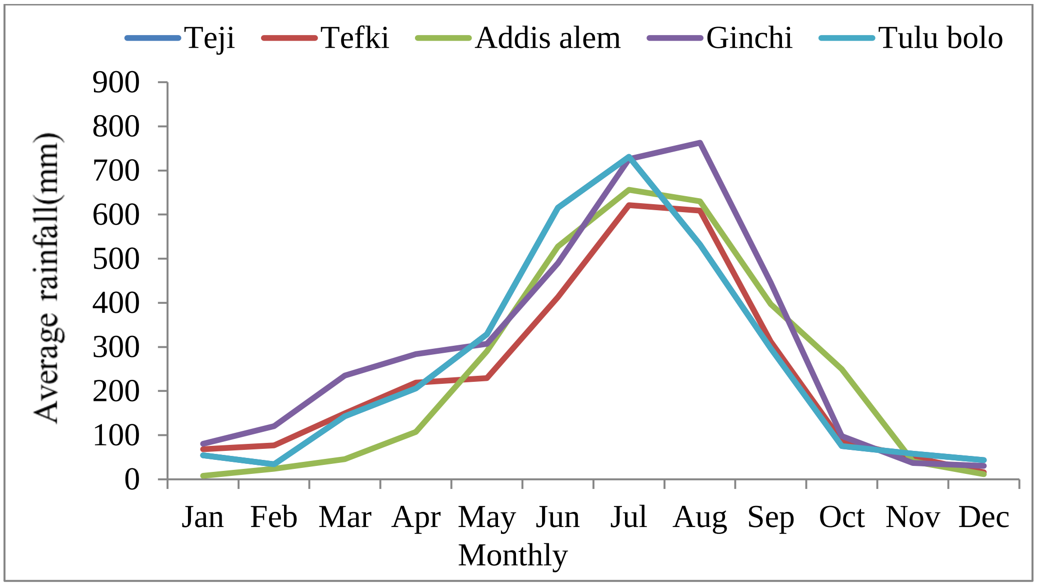

Figure 3.5 Mean monthly precipitation of stations in Awash Bello sub-basin (1990-2019)

3.4.1.2 Temperature Data

Temperature data is one of the most determinant meteorological data types. Failure of any thermometer or absence of an observer from a station causes a short break in the record of temperature at the station. The gaps should be estimated first before we use the temperature data for any analysis. Missing temperature data was filled using XLSTAT2015 software based on multiple imputation methods. As shown in (Figure 3.6), Awash Bello sub-basin obtains a mean monthly minimum and maximum temperature of the stations ranges from 7.75°C to 13.12°C and 21.8°C to 27.7°C respectively.

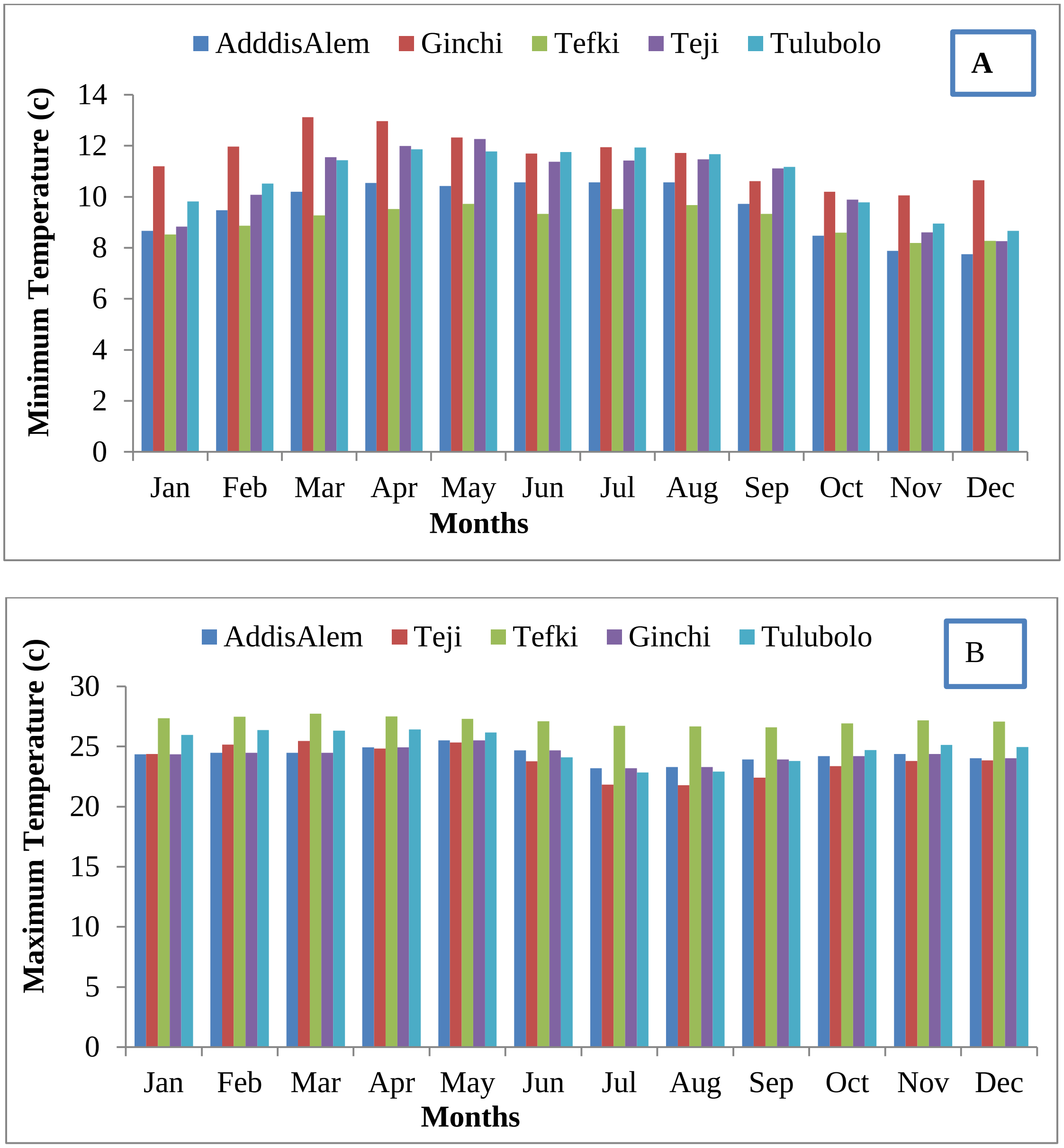

Figure 3.6 Mean monthly minimum (A) and maximum (B) temperature of stations in Awash Bello sub-basin stations

3.4.2 Data Quality Analysis

The raw data must be checked for qualities, which means that its continuity and consistency are used for further analysis. The quality control can be done by visual inspection, filling of missing data if there is any. This will help to identify if there are any gaps or unphysical peaks in the data series and correct them before the data is used or input into the model. Otherwise, using the inaccurate data as input to the model will give inaccurate output from the model.

3.4.2.1 Data Consistency test

Next to estimating missing precipitation, adjustment of the measured data is necessary to provide a consistent record. For checking the consistency of data Double mass curves were used. Double Mass Curve (DMC) analysis is a graphical method for identifying or adjusting inconsistencies in a station record by comparing its time trend with those of other nearby stations. In this method, the accumulated annual rainfall of a particular station is compared with the concurrent accumulated values of mean rainfall of groups of other surrounding base stations.

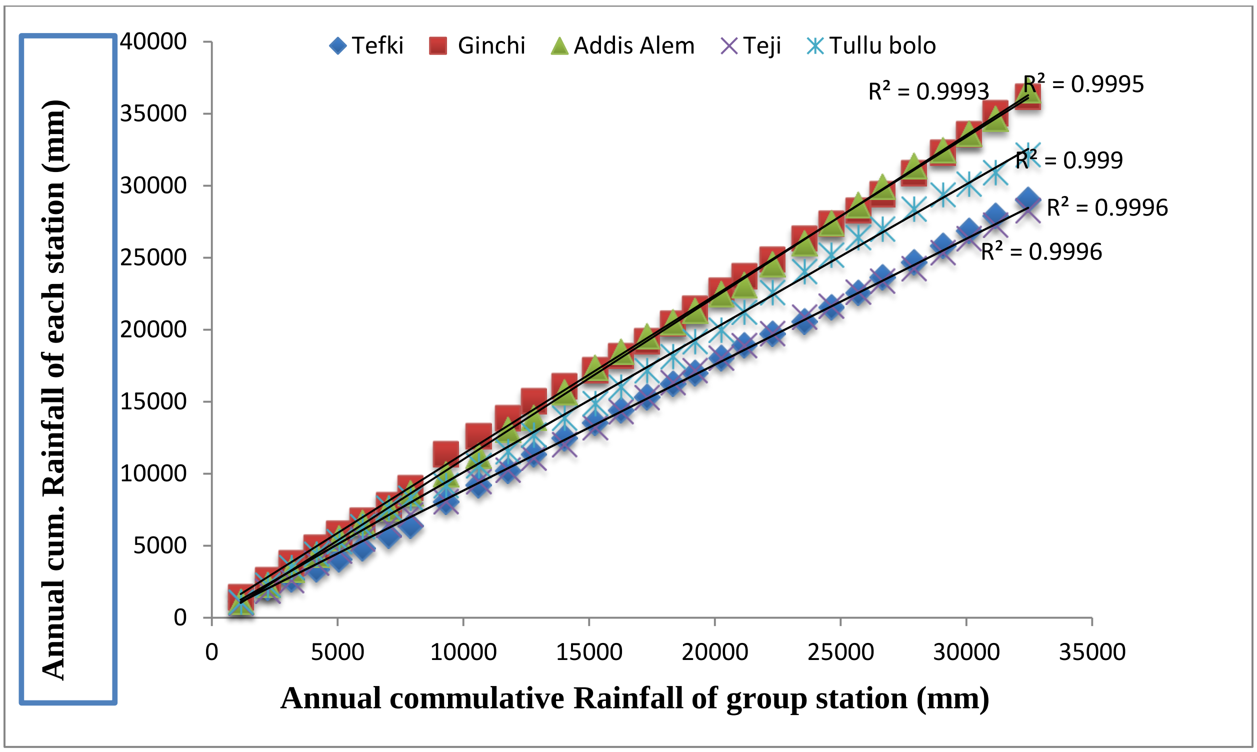

Figure 3.7 Rainfall consistency checking the result of selected meteorological stations

3.4.2.2 Rainbow Homogeneity Test

To test the homogeneity of the data set, Rainbow software was used to the Awash Bello sub-basin recording stations data. Analysis of rainfall data requires the data to be of long series; they should be homogeneous and independent. In RAINBOW, the test for homogeneity is based on the cumulative deviation from the mean (Raes, *et al*, 2006). Figure 3.8 shows the homogeneity test of the AddisAlem recording station. The probability of rejecting the homogeneity test is accepted at all significance levels (90, 95, and 99 %) for both ranges of cumulative deviation and maximum of cumulative deviation. Appendix B shows other stations' homogeneity test of annual rainfall.

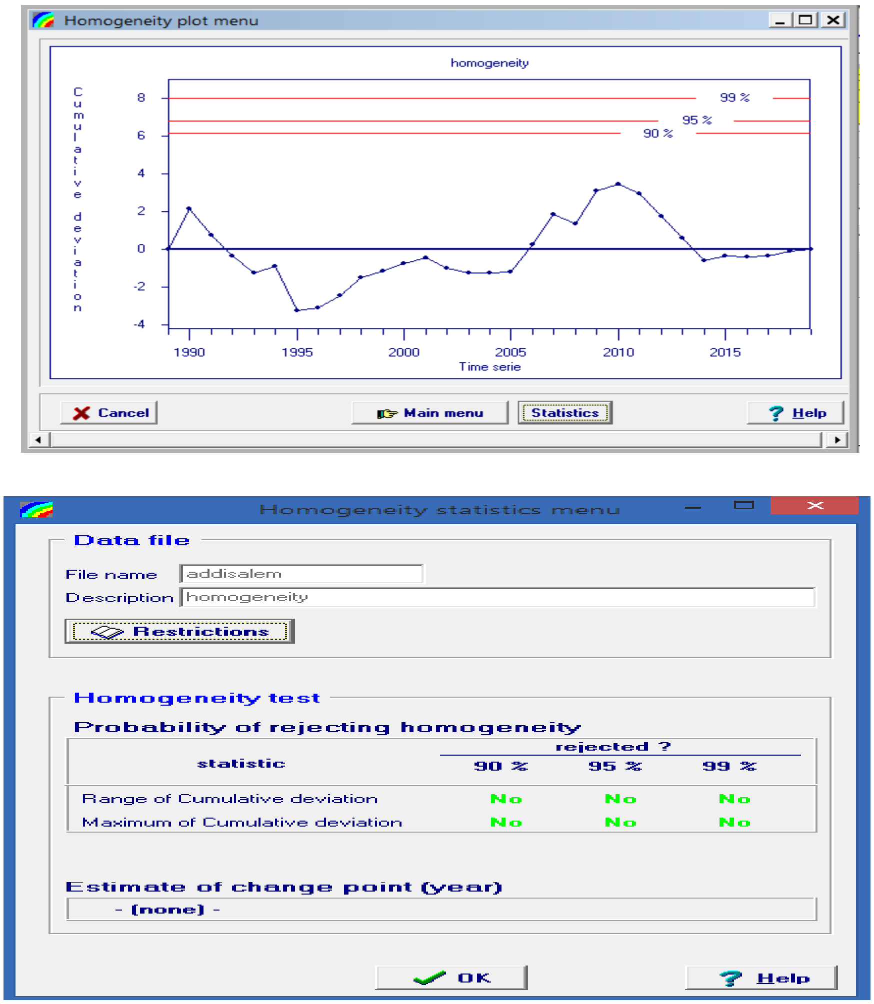

Figure 3.8 Cumulative deviation and probability of rejecting homogeneity test result of annual Rainfall at Addis Alem gauging station.

3.4.3 Estimating Areal Precipitation

Average rainfall over the catchment has been determined from the station measurements which are used in practical hydrological applications. Among the methods of determining areal rainfall, the Theissen polygon is the recognized one for computing areal precipitation. The method assumes that recorded rainfall in a gauge is representative of the area and also the adjacent gauged stations. The Theissen area is formed around each station by drawing the perpendicular bisectors of the lines joining adjacent stations using the ArcGIS tool. The polygons of the stations' areal contribution have been cropped using the shape of the catchments which includes stations of the selected ones for this study. The weighted average areal precipitation is found using the formula (Subarmaniya. 2008).

$$\overline{P} = \frac{\sum_{i=1}^{n} P_1 A_1}{\sum_{i=1}^{n} A_i} = \frac{[(P_1 \ A_1) + (P_2 \ A_2) + \ldots + (P_n \ A_n]}{[A_1 + A_2 + \ldots + A_n)]} \quad \text{...[3.1]}$$

Where; $\overline{P}$ areal precipitation, P is precipitation, A is the area of each site (meteorological stations), and n is the number of stations.

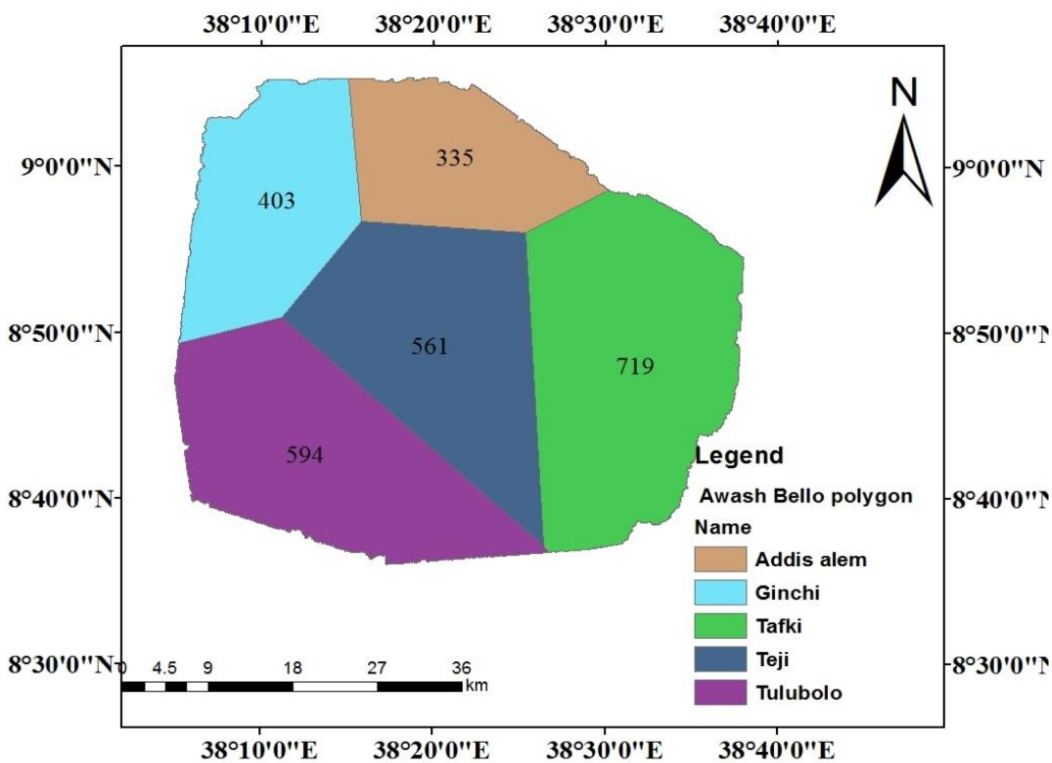

Figure 3.9 Theissen polygon of awash Bello sub-basin

3.4.4 RCM data analysis

The Downscaled Climate change data derived by HadGEM2-ES Global climate model outputs that are dynamically downscaled by the CORDEX-Africa program using RACMO22T regional model under representative concentration pathways (RCP4.5 and RCP8.5). Dibaba have report that RACMO22T to simulate rainfall over most stations better than the other models (Dibaba *et al.*, 2019). For this study, precipitation and maximum and minimum temperature datasets are downloaded from CORDEX and extracted using ArcGIS based on the grid points which are fitted to the meteorological stations in the study area and bias-corrected and the results are then compared to observed data. Relative humidity and solar radiation is remain constant. Representative Concentration Pathways (RCPs) of CMIP5 climate model output stands for a pathway to provide time-dependent projections of atmospheric greenhouse gas concentrations. This study uses the results for the moderate RCP4.5 and most extreme RCP8.5 emission scenarios. The HadGEM2-ES is a global climate model of the earth system category developed by the Hadley Centre of UK metrology office. The resolution is about 1.875 degrees in longitude and 1.275 degrees in latitude and 38 levels in the atmosphere (Yimer, 2018. It has a dynamic vegetation scheme with carbon cycle representation. The model supports the fifth phase of the Climate Model Intercomparison Project (CMIP5) (Jones *et al*., 2011). (Jilo, 2019) (Yimer, 2018) have used this model on the lower awash basin and Mille watershed.

3.4.4.1 Grid Selection for RCM data

The RCM output grid points of data have been classified based on their grid location (latitude and longitude). The grid selection has been carried out according to the location of the grid nearest distance concerning the location of each meteorological station that is selected for this study. Depending on their distance from the selected station five-grid cells were selected to the watershed. After grid point selection to the nearest station, the data has been extracted and bias correction has been computed for each selected grid value.

Table 3-2: Selected grid location nearest to the observed station in the Awash Bello sub-basin

Observed			RCM
Stations	LAT	LONG	Gridpoint nearest to each observed station
Ginchi	9.02	38.13	GP112214
Addis Alem	9.042	38.382	GP113215
Tulu bolo	8.67	38.22	GP113213
Teji	8.833	38.367	GP113214
Tafki	8.84	38.489	GP114214

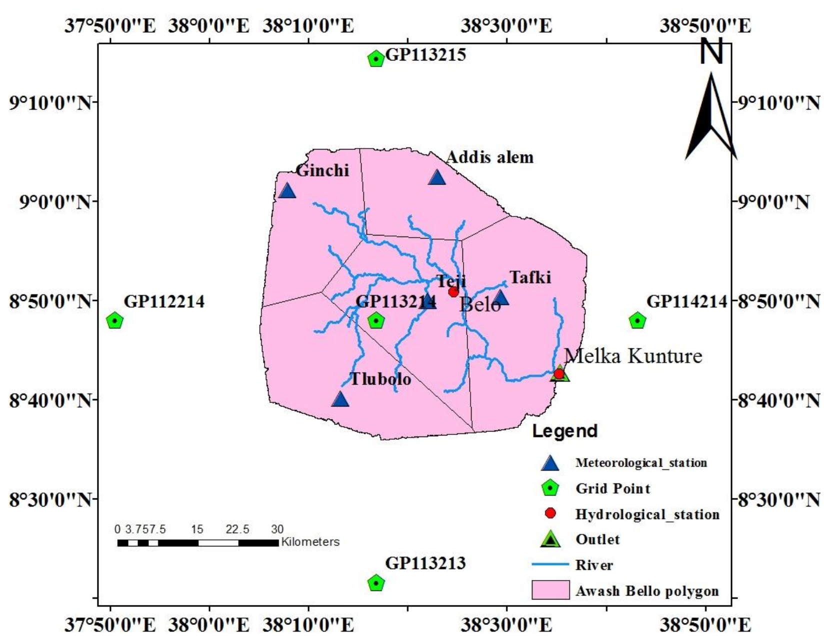

Figure 3.10 Awash Bello sub-basin selected meteorological stations with RCM grid points and hydrological gauge station locations.

3.4.5 Bias Correction

Bias correction methods are applied in climate impact studies to correct the climate input data provided by regional climate models for systematic statistical deviations from observation data (Muleta, 2021) . There are different types of bias correction methods for precipitation and temperature. In this study, Power Transformation for precipitation and Variance Scaling for Temperature were used. Therefore, these methods are most effective and recommend fitting our country's climate condition. This bias correction was used in previous studies like (Jilo, 2019) (Daba & You, 2020) (Muleta, 2021) (Kifle, 2020).

3.4.5.1. Bias corrected precipitation

The correction method is applied by comparing the daily observed precipitation at each station with the nearest grid point of the RCM considering the grid points as a single station on the watershed. The power transformation method is explained in equation 3.2.

$$P^* = a.P^b \quad \text{[3.2]}$$

Where P* is corrected precipitation, P is simulated precipitation. The parameters a and b is estimated by equalizing the coefficient of variation (CV) of the corrected simulations P^b and CV of the observed values, both from the calibration/optimization period. The value of a and b are shown in the appendex D.

At the monthly level, as shown in figure 3.11, some months have underestimated RCP precipitation as compared to the observed precipitation (March, April, June, July, and August), while the rest months are overestimated months (January, October, November, and December). However, the model simulates almost similar rainfall values observed during September and February before bias correction was applied. As is shown by Figure 3.11, before bias correction was applied, the difference between observed and simulated rainfall is large. However, after bias correction was applied, the graph of bias-corrected rainfall and observed rainfall values shows similar patterns and are close to each other. Figure 3.11 shows areal monthly precipitation of stations.

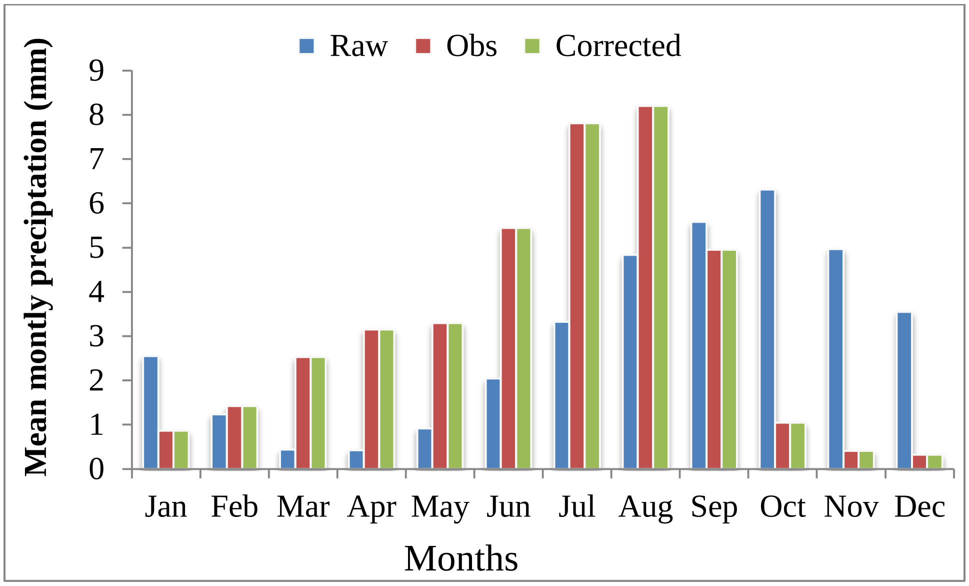

Figure 3.11 Comparisons between mean monthly Precipitation of Observed, bias-corrected RCM, and uncorrected (Raw RCM) of Awash Bello sub-basin stations.

3.4.5.2. Maximum Temperature

The variance scaling method was developed to correct both the mean and variance of normally distributed variables such as temperature (Teutschbein and Seibert, 2012). Temperature is normally corrected using the VARI method with equation 3.3.

$$T_{corr} = \overline{T}_{\text{obs}} + \frac{\sigma(T_{obs})}{\sigma(T_{rcm})} \left(T_{rcm} - \overline{T}_{rcm}\right) \quad \text{[3.3]}$$

Where T_{Corr}: the corrected daily temperature. T_{rcm}: the uncorrected daily temperature from RCM model and T_{obs}: the observed daily temperature while $\overline{T}_{obs}$ is the mean observed temperature and $\overline{T}_{rcm}$ is the mean simulated temperature.

The monthly maximum temperature of the selected climate model also underestimates maximum temperature before bias adjustment was applied and after bias was made on climate model, the graph shows a similar pattern with observed maximum temperature as shown in Figure 3.12 The result of bias correction shows that there is a satisfactory agreement between observed and simulated maximum temperature. The average maximum temperature of the model shows underestimation during all months except June and July. Observed, Uncorrected RCP, and bias-corrected areal mean monthly maximum temperature presented in figure 3.12.

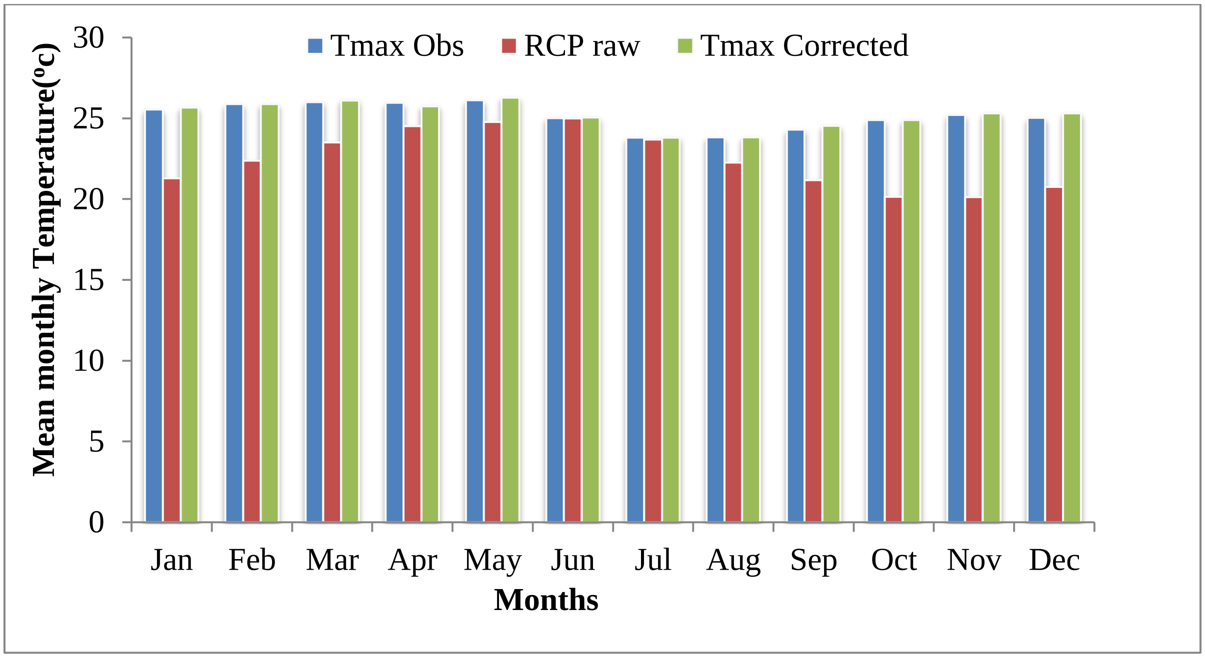

Figure 3.12 Mean monthly maximum temperatures of bias-corrected, uncorrected, and the observed of stations in Awash Bello sub-basin.

3.4.5.3 Minimum Temperature

Minimum Temperature is normally corrected using the VARI method with equation 3.3.

In the case of minimum temperature, the average minimum temperature shows that slight overestimation during June, July, August, September, and October, slight underestimation during January, February, March, April, and May, and the left months are similar. Like precipitation and maximum temperature, the bias correction minimum temperature shows a reasonably good agreement with the observed minimum temperature for all months. Figure 3.13 shows areal monthly minimum temperature of stations.

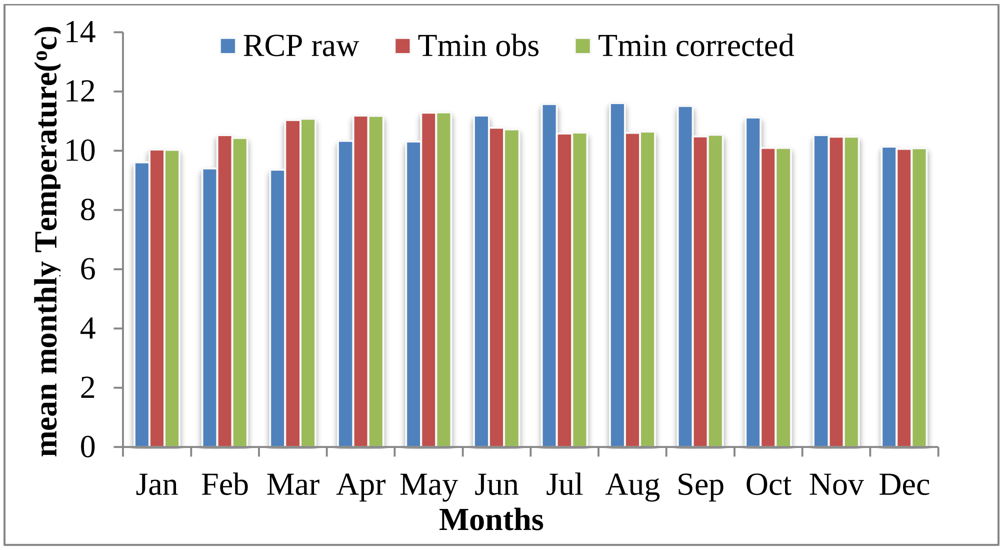

Figure 3.13 Mean monthly minimum temperature bias-corrected, uncorrected, and observed of stations of Awash Bello sub-basin.

3.5 SWAT Model Setup

3.5.1 Watershed delineation

Delineation of the watershed is the first step in creating SWAT model input using 12.5m by 12.5m resolution DEM data using ArcSWAT model watershed delineation function. Inputs entered into the SWAT model were organized to have spatial characteristics. Before going in hand with spatial input data i.e. the soil map, LULC map, and the DEM were projected into the same projection called UTM Zone 37N, which is a projection parameter for Ethiopia.

First, the SWAT project setup was created. The watershed delineation process consists of five major steps, DEM setup, stream definition, outlet and inlet definition, watershed outlets selection and definition, and calculation of sub-basin parameters (Nasiri *et al*., 2020). The size of sub-basins and the definition of streams were carefully determined by selecting the minimum drainage area required to shape the streams' origins (Geremew, 2013). Using a threshold value suggested by the ArcSWAT interface, the Awash Bello watershed was delineated into 35 sub-basins having an estimated total area of 2612 km^2. During the watershed delineation process, the topographic parameters (elevation, slope) of the watershed and its subwatershed were also generated from the DEM data. Accordingly, the elevation of the watershed ranges from 1988m to 2887m above mean sea level.

3.5.2 Hydrologic Response Units (HRU) Definition

Definition of HRU is the second step of the model setup. The SWAT model requires defining specific sub-basins called hydrologic response units, which consist of three elements: land use, soil types, and slope classification (Kalcic *et al.*, 2015). To determine the area and hydrologic parameters of each land-soil category simulated within each sub-watershed, the prepared land use, and soil maps, as well as their corresponding look-up tables, were loaded into the ArcSWAT interface for reclassification using SWAT coding standards (Megersa *et al*., 2019). The look-up table was used to describe the land cover/land use classes that identify the four-letter SWAT code for each category of land cover/land use, allowing the grid values to be connected to SWAT land cover/land use groups. After code was assigned to all map types calculations of the area covered by each land use and reclassification were done.

The DEM data that was used to define the watershed was also used to classify the slopes (Megersa *et al*., 2019). After the reclassification of the land use, soil and slope grids overlay operations were performed to create HRU areas that had similar hydrological conditions. Thresholds from 5% to 15% are commonly used (Her *et al*., 2015). For this specific study, based on her report, a threshold value of 5% for land use, 10% for soil, and 10% for slope were used. Since the sub-basins have such a large range of slopes, the multiple slope variation was preferred over the single slope variation. Finally, the HRU definition was completed. In this analysis, the HRU distribution was determined by assigning several HRU to each sub-basin below the threshold level that excludes minor land uses, soils, and slope grades. Following the elimination process, the remaining land use, soil, or slope class's area was redistributed so that 100% of land area in the sub-basin was modeled.

The overall watershed delineation and HRU definition simulation in this analysis resulted in a 2612km^2 watershed with 35 sub-basins and 218 HRUs. The minimum, maximum, and mean elevations in the sub-basin were 1988m, 2887m, and 2437.5m (a.m.s.l) respectively, according to the watershed delineation of the area.

In this study, multiple slope options (an option for considering different slope classes for HRU definition) were selected and the slope class was classified into three and the range was 0-3%, 3-6%, and above 6% in Figure 3.14.

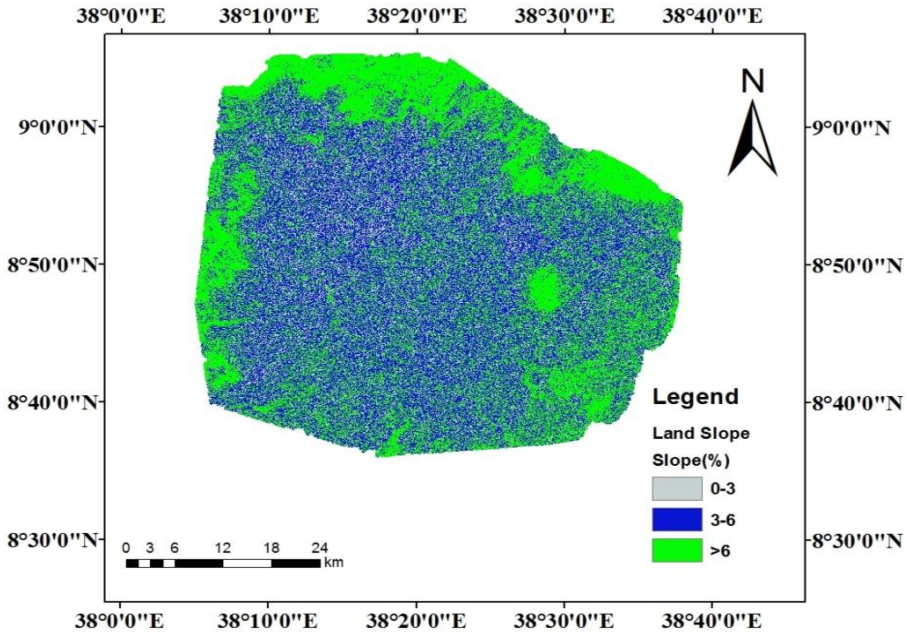

Figure 3.14 slope of Awash Bello sub-basin

3.5.2.1 Land Use /Cover and Soil Data

The land use land cover map gives the spatial extent and classification of the various land use land cover classes of the study area. The land use condition in the Awash Bello sub-basin includes mainly moderately cultivated, intensively cultivated, Eucalyptus woodland, dense coniferous high forest, and Open grassland. Similarly, the Awash Bello sub-basin consists of different soil types among which pellic vertisols cover more than 80% of the area and Orthic Solonchaks follows the second rank. Generally, the land use/cover and soil type of the Awash Bello sub-basin with percent of coverage is indicated in table 3.3 and 3.4 below.

Table 3-3 Land use land of Awash Bello sub-basin (2013)

LULC types	SWAT code	Area (km^2)	% age area
Moderately cultivated	TEFF	251.524	9.63
Intensively cultivated	AGRL	2272.46	87.00
Eucalyptus woodland	FRSD	14.3478	0.55
Dense coniferous high forest	RNGE	67.7314	2.59
Open grassland	FRSE	5.8652	0.23

Table 3-4 Soil type of Awash Bello sub-basin

SOIL TYPE	**SWAT code**	**Area (km^2)**	**% cover**
calcic xerosols	Lf31-a-1453	2.72	0.10
chromic cambisols	Be54-2-3a-454	30.20	1.16
chromic luvisols	Nh7-2-3c-853	38.00	1.46
chromic vertisols	Nd17-1a-1554	31.24	1.20
dystric nitisols	Vc39-3a-955	14.76	0.57
eutric cambisols	Be56-2-3a-456	148.73	5.69
eutric fluvisols	Fo94-2ab-556	0.02	0.00
eutric nitisols	Vc40-3a-956	86.69	3.32
Leptosols	I-Jc-Xk-2-71	2.52	0.10
orthic solonchaks	I-Lf-Rd-1264	167.08	6.40
pellic vertisols	Nd3-1565	2089.96	80.00

3.5.3 Weather Generator

SWAT uses the WXGN weather generator to generate or fill weather information using user-specified statistics of rainfall, temperature, solar radiation, wind speed, and dew point temperature. The WXGN weather generator is a statistical model that uses numerous core weather statistics (defined for each month) to generate synthetic weather data (Ghimire *et al.*, 2019). The swat model has an automatic weather data generator. However, it needs some input data to run the model. The input data required are daily values of precipitation, maximum and minimum temperature, solar radiation, wind speed, and relative humidity. But, in many areas, such data are either records may not have sufficient length or incomplete, which is the case in this study. If no data is available at the same time for all stations, the model can generate all the remaining data from daily precipitation and temperature data.

Some programs are used to provide generator such as pcpSTAT and Dew02.exe to calculate daily statistical parameters of precipitation like PCPMM, PCPSKW, PR_W1, PR_W2, and PCPD and to calculate average daily dew point temperature per month using daily air temperature (dewt) and humidity data respectively which are assigned in one row in excel to make it compatible with the SWAT database (Akpoti, 2016b) (Daba, 2017). In this study, five stations are used to run the SWAT model, and Ginchi meteorological station was used as an automatic weather data generator for the rest of the missing in the Awash Bello sub-basin.

3.5.4 Weather Data Input Definition

Following the watershed delineation and HRU definition, the next step was writing the input table. This section includes batch files that contain longitude, latitude, and elevation of weather generator rainfall, temperature, relative humidity, solar radiation, and wind gauge stations and it was loaded sequentially. As a result, available weather data from AddisAlem, Ginchi, Tefki, Teji, and Tulu bolo meteorological stations were used. Then, for each sub-basin, SWAT cells each meteorological data file and writes it to the database.

3.6 SWAT Model Simulation

After the SWAT model setup was completed, the next step was SWAT model simulation (Nasiri *et al*., 2020). To simulate the model it is required to set the start and end dates, printout settings, and warming times, then run the model and the result of SWAT output files used for various analysis, while the result cannot be used for further analysis directly. Instead, the ability of the model to sufficiently predict the consistent streamflow should be evaluated by sensitivity analysis calibration and validation of the model. Generally, the simulation was performed for thirty years of recording periods starting from 1990-2019, for baseline and 2021-2050 to 2051-2080 for the middle term and far-term period under RCP4.5 and RCP8.5.

3.6 SWAT Model Sensitivity Analysis, Calibration, and Validation

3.6.1 Sensitivity Analysis

The sensitivity analysis aims to estimate the rate of change in the output of a model concerning changes in watersheds that result in a clear difference in hydrologic sensitivity (Reungsang *et.al*, 2005). Sensitivity analysis reduces uncertainty by determining the relative ranking of which parameters have the greatest impact on output variance due to input variability. The sensitivity ranking, as well as testing their t-stat, which provides a measure of sensitivity (larger absolute values indicate greater sensitivity), and p values, which determine the significance of the sensitivity (a value close to zero has more significance) (Tufa & Sime, 2020).

For enormous hydrological models like SWAT, which involves a wide range of data and parameters in the simulation process, calibration is quite a bulky task. Even though it is quite clear that the flow is largely affected by curve number, for example in the case of the SCS curve number method, this is not sufficient enough to make calibration as little change in other parameters could also change the volumetric, spatial, and temporal trend of the simulated flow. Hence, sensitivity analysis is a method of minimizing the number of parameters to be used in the calibration step by making use of the most sensitive parameters largely controlling the behavior of the simulated process (Reay *et al*., 2007). This appreciably eases the overall calibration and validation process as well as reduces the time required for it.

After a thorough pre-processing of the required input for the SWAT 2012 model, flow simulation was performed for thirty years of recording periods starting from 1990 through 2019. Sensitivity analysis was performed on 17 SWAT parameters (SCS curve number (R_CN2), Baseflow Alfa factor (V_ALPHA_BF), Groundwater delay (days) (V_GW_DELAY), Groundwater"revap" coefficient (V_GW_REVAP), Soil evaporation compensation factor (V_ESCO), Effective hydraulic conductivity in channel (V_CH_N2), sol Available soil water capacity (R_SOL_AWC), Soil hydraulic conductivity (V_SOL_K), Snowfall temperature (V_SFTMP), Threshold depth of water in the shallow aquifer for "revap" to occur (mm) (R_REVAPMN), Manning's "n" value for overland flow (R_OV_N), Average slope steepness (R_HRU_SLP), surface runoff lag time (R_SURLAG), effective hydraulic conductivity in main channel alluvium (V_CH_K2) threshold depth of water in the shallow aquifer required for return flow to occur (mm) (V_GWQMN), deep aquifer percolation fraction (R_RCHRG), and Moisture bulk density (R_SOL_BD) and the most sensitive parameters were identified using the Global sensitivity analysis method in SWAT-CUP SUFI12 (Griensven, 2005). The codes R, and V are types of change that applied to the parameter in the model. R represents existing parameter value is multiplied by 1+ a given value and V represent the default value to be replaced by a given value (Akpoti, 2016b) (Akpoti, 2016a). The selection of sensitivity analysis is based on runoff, sediment, and nutrient and pesticides (Arnold, *et al*, 2012).

3.6.2 Calibration and Validation

Calibration involves testing the model with known input and output data to adjust some parameters, while validation involves comparison of the model results with an independent dataset during calibration without any further adjustment of the calibration parameters.

There are various sources of uncertainties that were related to data, model assumptions, and RCM output. After finding the sensitive parameters on streamflow simulation, the SUFI-2 algorithm was used in SWAT-CUP to calculate the calibration and validation parameters (Abbaspour, 2015). Then, the calibration periods were defined from 2000 to 2010 and the validation period from 2011 to 2016. SUFI-2 algorithms gave good results in minimizing the differences between observed and simulated flow in the Awash Bello sub-basin.

3.7 SWAT Model Performance Evaluation

Model evaluation is an essential measure to verify the performance of the model. There are various methods to evaluate the model performance during the calibration and validation periods. For this study, three methods were used. These were coefficient of determination (R^2), percentage of BIAS, and Nash and Sutcliffe simulation efficiency (NSE).

The determination coefficient (R^2) describes the proportion of the variance in measured data by the model. It is the magnitude linear relationship between the observed and the simulated values. R^2 ranges from zero (which indicates the model is poor) to one (which indicates the model is good), with higher values indicating less error variance, and typical values greater than 0.6 are considered acceptable (Santhi *et al*., 2001). The model performance in simulating observed discharge was evaluated during calibration and validation by the three performance indicators:

Nash and Sutcliffe efficiency (NSE $\geq$ 0.5), coefficient of determination, ($R^2 \geq$ 0.6), and PBIAS $\leq$ $\pm$ 25% (Kazi, *et al*, 2019).

The coefficient of determination, R^2 is estimated by the equations below;

$$R^2 = \left(\frac{\Sigma(Q_{obs} - \overline{Q}_{obs})^2 - \Sigma(Q_{sim} - \overline{Q}_{sim})^2}{\Sigma(Q_{obs} - Q_{obs})^2}\right) \text{..........}[3.3]$$

The Nash-Sutcliffe Efficiency (NSE) simulation coefficient was used to analyze the agreement between the time verse flow plot of the observed and simulated values (Ayele *et al*., 2017). As defined by equation 3.2.

$$NSE = 1- \frac{\sum_{i=1}^{n}(Q_{obs} - Q_{sim})^2}{\sum_{i=1}^{n}((Q_{obs} - \overline{Q_{obs}}))^2} \text{..........} [3.4]$$

Over a specified period (usually the entire calibration or validation period), the percent difference or percent bias (PBIAS) defines the tendency of the simulated data to be greater or smaller than the observed data values. This is determined by equation 3.3.

$$PBIAS\ (\%) = \frac{\sum_{i=1}^{n}(Q_{obs} - Q_{sim}) * 100}{\sum_{i=1}^{n} Q_{obs}} \text{..........}[3.5]$$

Where Q_{obs} is observed discharge, Q_{sim} is simulated discharge, $\overline{Q}_{obs}$ is mean the of observed discharge and, $\overline{Q}_{sim}$ is the mean of simulated discharge.

3.8 Future Climate Change Scenarios

A climate scenario is a plausible image of a future climate based on knowledge of the past climate and assumptions on future change (an increase of greenhouse gas (GHG) concentrations (Dierickx, 2019). It refers to probably future climate that has been constructed for explicit use in investigating the potential consequence of anthropogenic climate change (Hayhoe *et al*., 2017). Climate change scenarios are developed to give coherent, internally consistent, and plausible descriptions of the future state of the world. The climate change scenarios should be assessed according to consistency with global projections, physical plausibility, applicability in impact assessments, and representatively (Abera, 2011). It is largely the uncertainty surrounding this assumption that determines the range of possible scenarios (Mammo, 2017).

Emissions scenarios are descriptions of potential future releases to the atmosphere of substances that affect the Earth‘s radiation balance, such as greenhouse gases and aerosols (Bjornaes & Ni, 2015). Representative Concentration Pathways (RCPs) are the four new greenhouse gas concentration trajectories included by the IPCC, 2014 in its fifth Assessment Report (AR5) (Pachauri, 2014). The words concentration pathway are meant to emphasize that these RCPs are not the final new, fully integrated scenarios (i.e. they are not a complete package of socio-economic, emission, and climate projections), but instead are internally consistent sets of projections of the components of radiative forcing that are used in subsequent phases (van Vuuren et al., 2011). A new set of scenarios, the Representative Concentration Pathways (RCPs), was used for the new climate model simulations carried out under the framework of the Coupled Model Intercomparison Project Phase 5 (CMIP5) of the World Climate Research Program. A large number of comprehensive climate models and ESMs have participated in CMIP5, whose results form the core of the climate system projections (Stocker *et al*., 2013). These define four likely climate futures in the coming years which are considered potential depending on the amount of emitted greenhouse gases.

They are not always used for the construction of regional climate scenarios. RCP2.6 is considered less applicable, RCP4.5 and RCP6.0 are intermediate climate scenarios while RCP4.5 is used for intermediate scenarios because it is often used to indicate the lower probable climate change but RCP6.0 is not used much in the scenarios as it does not necessarily add much additional information when showing the range of possible climate change, RCP8.5 represents the highest emissions and consequently the largest climate change (it was often referred to as worst-case) (Dierickx, 2019). In this study, climate change scenarios data from the newly available CMIP5, RCM output of CORDEX Africa for African domain projections under Representative Concentration Pathways (RCP4.5 and RCP8.5) was used as input to the hydrological model. RCP scenarios have a better resolution that helps in performing regional and local comparative studies compared to previous climate scenarios. For this study RCP4.5 and RCP8.5 are selected because RCP4.5 is a modest scenario in which radiative forcing stabilized by 2100 and RCP8.5 assumes a worst-case scenario with the least amount of effort in emissions reductions (Bjornaes & Ni, 2015).

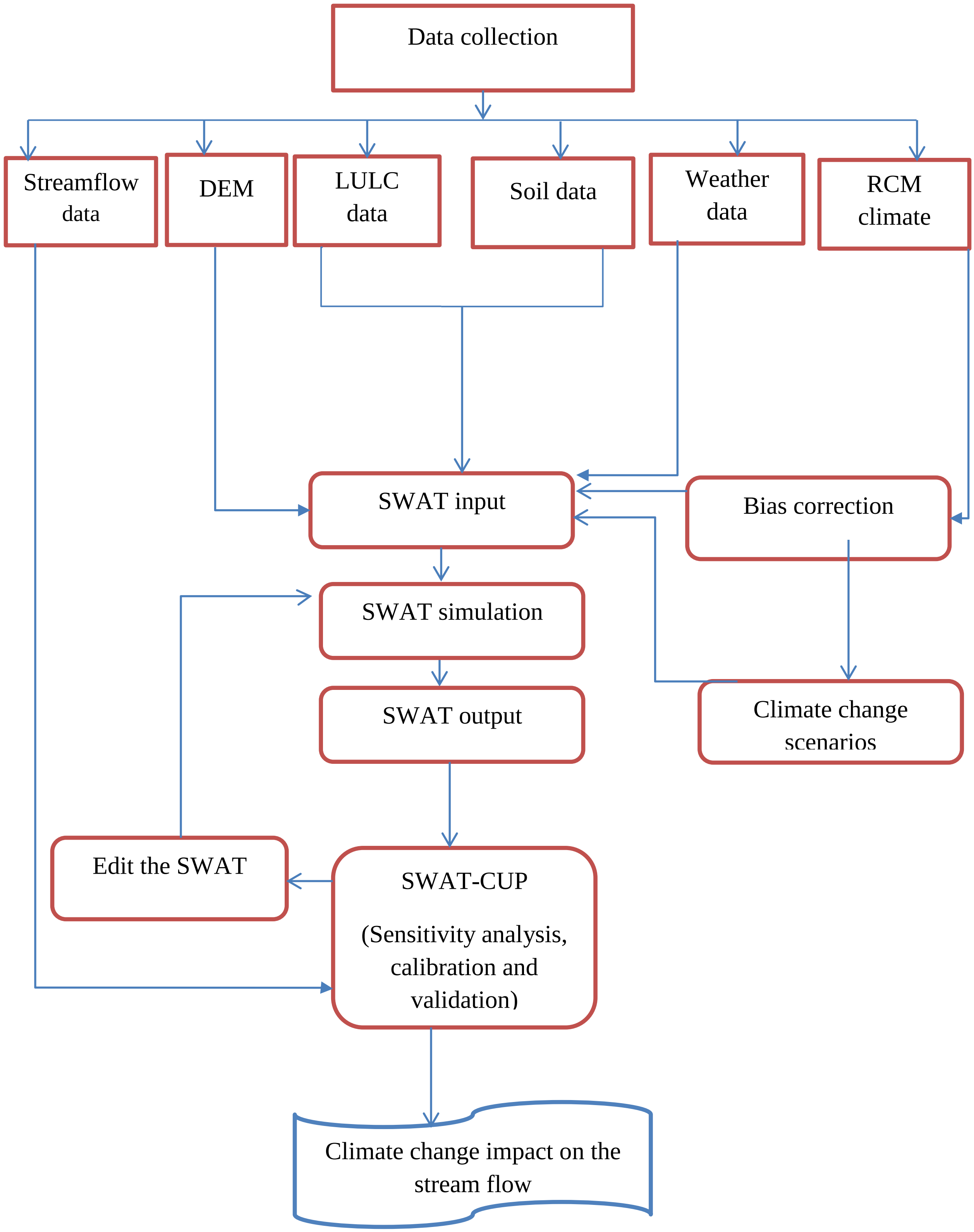

Figure 3.15 conceptual framework of the study

4. RESULTS AND DISCUSSIONS

4.1 Future projection of climate change

For this study $0.44^0 * 0.44^0$ grid resolutions of RCM model outputs based on RCP4.5 and RCP8.5 emission scenarios were used for analysis. The future climate data includes precipitation and maximum and minimum temperature. The Projected future scenarios have been divided into two consecutive (30) years. Therefore, the period from 1990-2019 taken as a base period and two future periods considered for impact analysis of the 2050s (2021-2050) and 2080s (2051-2080).

4.1.1 Future projection of Climate Impacts on Precipitation

The future projected changes in precipitation data are important means of evaluating the features of precipitation at the sub-basin. The seasonal and annual rainfall distribution patterns for all bias-corrected RCM were shown in figure 4.1 below

The projected seasonal and annual precipitation change under RCP4.5 and RCP8.5 scenarios was analyzed in this study. The seasonal percentage change for two future projection periods under the two emission scenarios has shown in figure 4.1 below. The result indicated that seasonal precipitation in the Belg (FMAM) in a minor rainy season is expected to increase by +2.28% and +1.78% under RCP4.5 and RCP8.5 for (2021-2050) and decrease by -13.63% and -12.25% under both scenarios for (2051-2080). In Bega (ONDJ) dry season, there would be a decrease in seasonal precipitation within the interval (-14.66% to -31.49%) under both time horizons and scenarios. However, during Kiremt (JJAS) major rainy season, there would be an increase in seasonal precipitation for all seasons within ranges +19.06% to +29.15% under RCP4.5 and RCP8.5 emission scenarios for 2021-2050 and 2051-2080 periods.

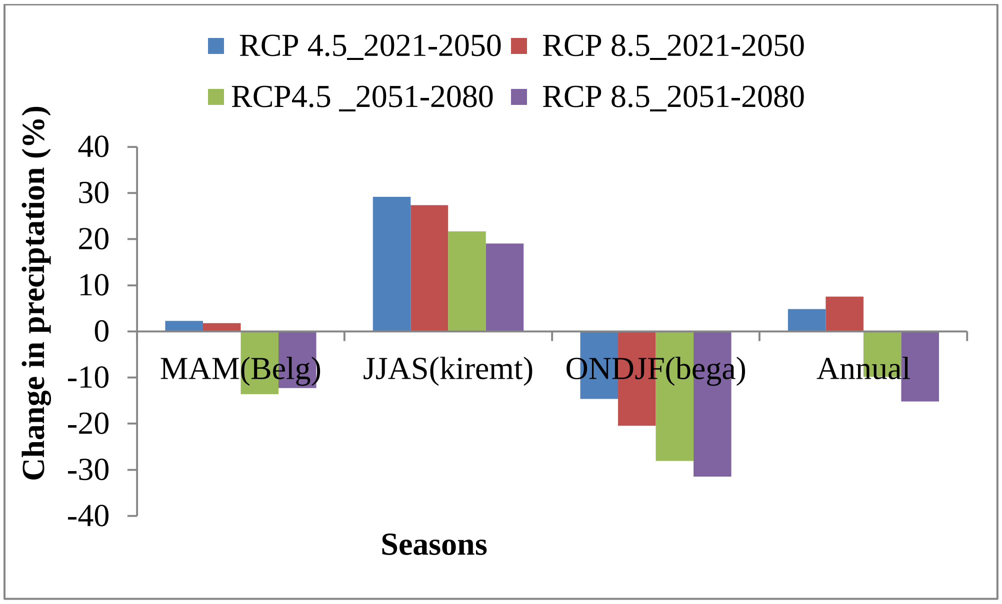

Figure 4.1 Seasonal and annual precipitations under RCP4.5 and RCP8.5 for 2021-2050 and 2051-2080

For the annual mean precipitation change result shown in the future precipitation, there would be an increase of +4.85% and +7.56% for the period of (2021-2050) under RCP4.5 and RCP8.5 emission scenarios respectively. For (2051-2080) time horizons projected annual precipitation expected to decrease by -9.87% and -15.21% under RCP4.5 and RCP8.5 emission scenarios. The finding of (Getahun, 2020) and (Daba & You, 2020) for the upper awash sub-basin agreed with these results.

4.1.2 Future Projection of Climate Impacts on Minimum Temperature

The projected change in the mean monthly minimum temperature under RCP4.5 and RCP8.5 scenarios for the baseline period is shown in (Fig.4.2 below for both time horizons.

The projected seasonal minimum temperature in Kiremt (JJAS) major rainy season the minimum temperature expected to increase under both emission scenarios by (0.9^{o}c and 0.83^{o}c) and (1.23^{o}c and 1.34^{o}c) for 2021-2050 and 2051-2080 periods under RCP4.5 and RCP8.5 emission scenarios respectively. In Bega (ONDJ) dry season all projection periods are expected to increase within the range between 0.81^{o}c to 1.5^{o}c for both period and scenarios. In Belg (FMAM) minor rainy season minimum temperature of all projection periods would be expected to increase within the range 0.83^{o}c to 1.4^{o}c for both periods and emission scenarios. Likewise, annual average temperature showed an increasing trend by 0.78^{o}c to 1.38^{o}c for all scenarios (RCP4.5 and RCP8.5) for both projection periods. The previous studies on the awash basin show an increase in minimum temperature. The result of (Jilo, 2019) and (Bekele *et al.*, 2019) argued that the annual minimum would increase under RCP4.5 and RCP8.5 scenarios.

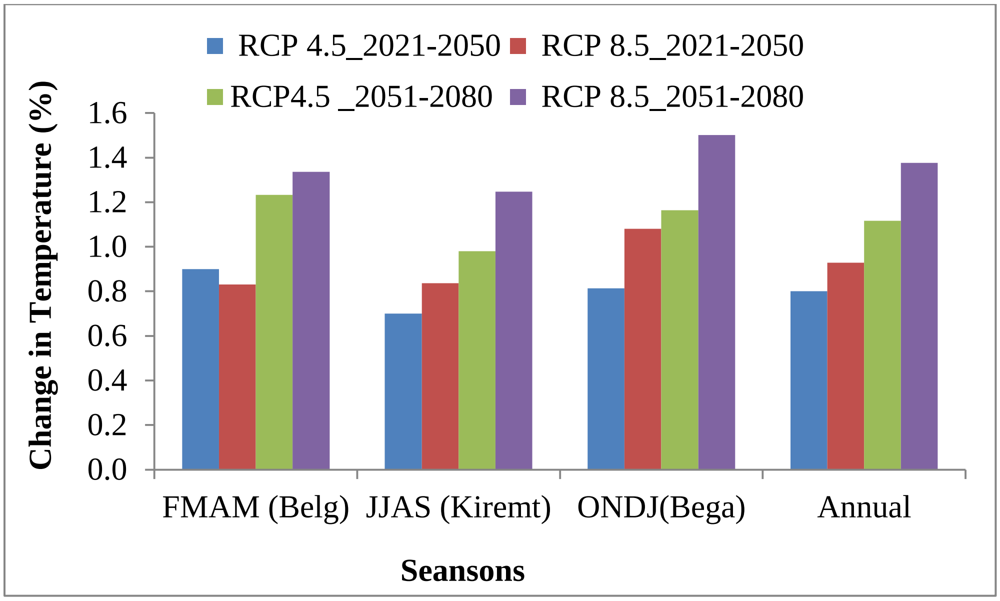

Figure 4.2 seasonal and annual minimum temperature changes for 2021-2050 and 2051-2080 of RCP4.5 and RCP8.5

4.1.3 Future Projection of Climate Impacts on Maximum Temperature

The projected change in the seasonal maximum temperature under RCP4.5 and RCP8.5 scenarios for the baseline period as shown in (Fig.4.3) below, the maximum temperature shows an increment for both time horizon and emission scenarios.

The projected annual maximum temperature in Kiremt (JJAS) major rainy season the maximum temperature expected to increase under both emission scenarios by (1^{o}c and 1.04^{o}c) and (1.2^{o}c and 1.28^{o}c) for 2021-2050 and 2051-2080 periods under RCP4.5 and RCP8.5 emission scenarios respectively. In Bega (ONDJ) dry season all projection periods are expected to increase within the range between 1.03^{o}c to 1.49^{o}c for both period and scenarios. In Belg (FMAM) minor rainy season maximum temperature of all projection periods is expected to increase within the range of 1.12^{o}c to 1.46^{o}c for both periods and emission scenarios. Likewise, annual maximum temperature showed an increasing trend by 1.06^{o}c to 1.43^{o}c for all scenarios (RCP4.5 and

RCP8.5) for both projection periods. Previous studies like (Sab-basin & Daba, 2018) (Bekele *et al.*, 2019), and (Jilo, 2019) have also argued that maximum temperatures would increase under RCP4.5 and RCP4.5 scenarios.

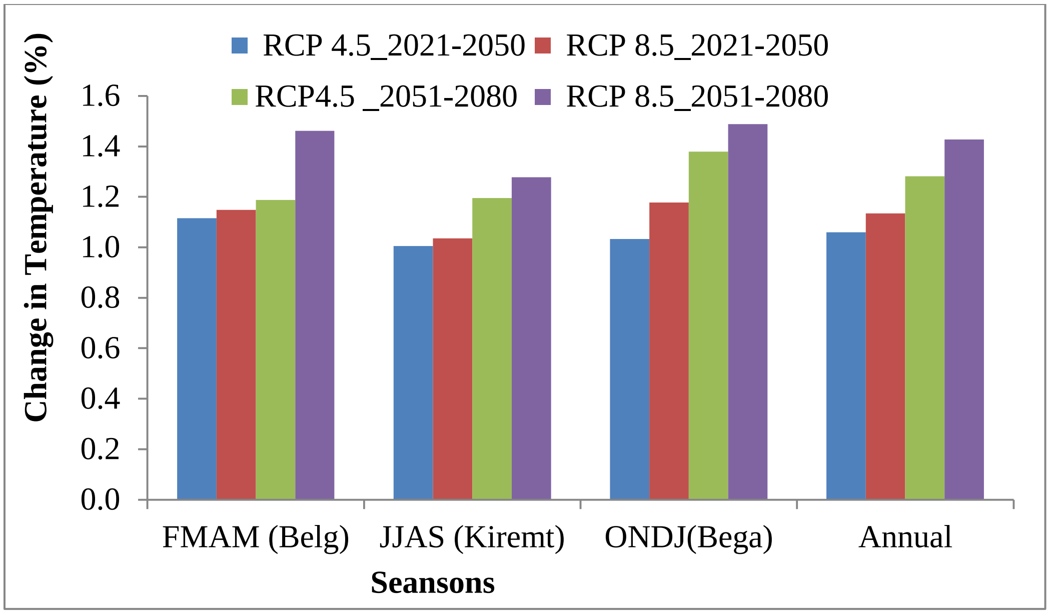

Figure 4.3 seasonal and annual maximum temperature changes for 2021-2050 and 2051-2080 of RCP4.5 and RCP8.5

4.2 Evaluating the performance of the SWAT model

To evaluate the accuracy of SWAT simulation performance, the coefficient of determination (R^2), the Nash and Sutcliffe model efficiency coefficient (NSE), and percentage bias (PBAIS) were used. The statistical results of the model's calibration were and for validation. The calibrated model was then used to validate the model from 2000 to 2016. The data analysis showed that the observed and simulated streamflow had been in strong agreement, with R^2 values which are summarized in table 4.1. Figure 4.3 and figure 4.5 show a graph of simulated and observed streamflow during calibration and validation. A scatter plot of simulated and observed streamflow of Melka kunture with the best-fit line having a correlation coefficient of 0.89 for calibration and 0.88 for validation was shown in figure 4.6.

The findings showed that observed and simulated monthly streamflow were in strong agreement. The model previously performed well at the Mojo river subwatershed, which is located in the upper awash river basin (Amin & Nuru, 2020). The ArcSWAT model was calibrated and tested by several authors, and their findings show that the statistical parameters (R^2 and NSE) ranged between 0.6 and 0.9 (Dibaba *et al*., 2020) (Sime *et al*., 2020) (Gessesse *et al*., 2019) (Tufa & Sime, 2020). Therefore, the ArcSWAT model can be used in the Awash River Basin in general and the Awash Bello sub-basin in particular. The simulated values in this study are acceptable.

4.2.1 Sensitivity Analysis

Sensitivity analysis is used to identify the model parameters that exert the highest influence on model calibration or model predictions. Sensitivity analysis was performed on flow parameters of SWAT on monthly time steps with observed data of the Malka Kunture gauge station. For this analysis, 17 parameters were considered and only 12 parameters were identified to have significant influence in controlling the streamflow in the watershed. The most sensitive parameter was found to be CN2 (Initial SCS runoff curve number for moisture condition II), followed by ALPHA_BF.gw (Base flow Alfa factor), GW_ REVAPMN (Threshold depth of water in shallow aquifer for revap or percolation to the deep aquifer), etc.

Table 4-1 Sensitivity ranking of parameters towards water flow

Parameter Name	t-Stat	P-Value	Rank
R__CN2.mgt	-4.269	0.000	1
V__ALPHA_BF.gw	1.645	0.109	2
V__GW_REVAP.gw	0.966	0.340	3
R__HRU_SLP.hru	-0.663	0.511	4
:R__SOL_AWC(..).sol	-0.658	0.515	5
V__ESCO.hru	-0.612	0.544	6
V__SFTMP.bsn	0.478	0.636	7

R__SOL_K(..).sol	-0.436	0.666	8
V__CH_N2.rte	0.269	0.790	9
R__REVAPMN.gw	0.238	0.813	10
V__GW_DELAY.gw	-0.102	0.919	11
R__OV_N.hru	0.040	0.968	12

Table 4-2 Flow sensitive parameters and fitted values

Parameter Name	**Description**	Fitted_Value	Min_value	Max_value
R__CN2.mgt	SCS curve number	0.035	-0.2	0.2
V__ALPHA_BF.gw	Baseflow Alfa factor	0.83	0	1
V__GW_DELAY.gw	Groundwater delay (days)	34.200001	30	450
V__GW_REVAP.gw	Groundwater ”revap” coefficient	0.0921	0.09	0.3
V__ESCO.hru	Soil evaporation compensation factor	0.01	0	1
V__CH_N2.rte	Effective hydraulic conductivity in channel	0.2003	0.11	0.32
R__SOL_AWC.sol	Available soil water capacity	0.268	0	0.4
R__SOL_K.sol	Soil hydraulic conductivity	0.472	0	0.8
V__SFTMP.bsn	Snowfall temperature.	2.05	0	5
R__REVAPMN.gw	Threshold depth of water in the shallow aquifer for ”revap” to occur (mm)	39.700001	10	100
R__OV_N.hru	Manning’s “n” value for overland flow	15.900001	0	30
R__HRU_SLP.hru	Average slope steepness	0.042	0	0.2

4.2.2 Model calibration and validation

After identifying the most sensitive parameters, the selected model parameters values were changed iteratively within a reasonable range during several calibration runs until attaining satisfactory agreement between observed and simulated streamflow. Awash Bello watershed gauging station recorded stream data at the outlet of Awash Bello sub-basin used for calibration and validation of the model. The daily streamflow data available for calibration and validation was 17 years (2000–2016) which is Streamflow data of 11 years (2000–2010) used for calibration and streamflow data of 7 years (2011–2016) used for validation. The results of these tests illustrated that the monthly coefficient of determination (R^2), Nash Sutcliff efficiency

(NSE), and PBIAS were 0.89, 0.87, and -11.9 for the calibration period, 0.88, 0.86, and -17.1 for the validation period. The result of calibration and validation for the monthly flow hydrograph showed that there is a good agreement between the measured and simulated monthly flows.

Table 4-3 Model efficiencies parameters in calibration and validation periods

Performance measure	**Calibration (2000-2010)**	**Validation (2011-2016)**
Coefficient of determination (R^2)	0.89	0.88
Nash Sutcliff efficiency (NSE)	0.87	0.86
Pbias	-11.9	-17.1

.

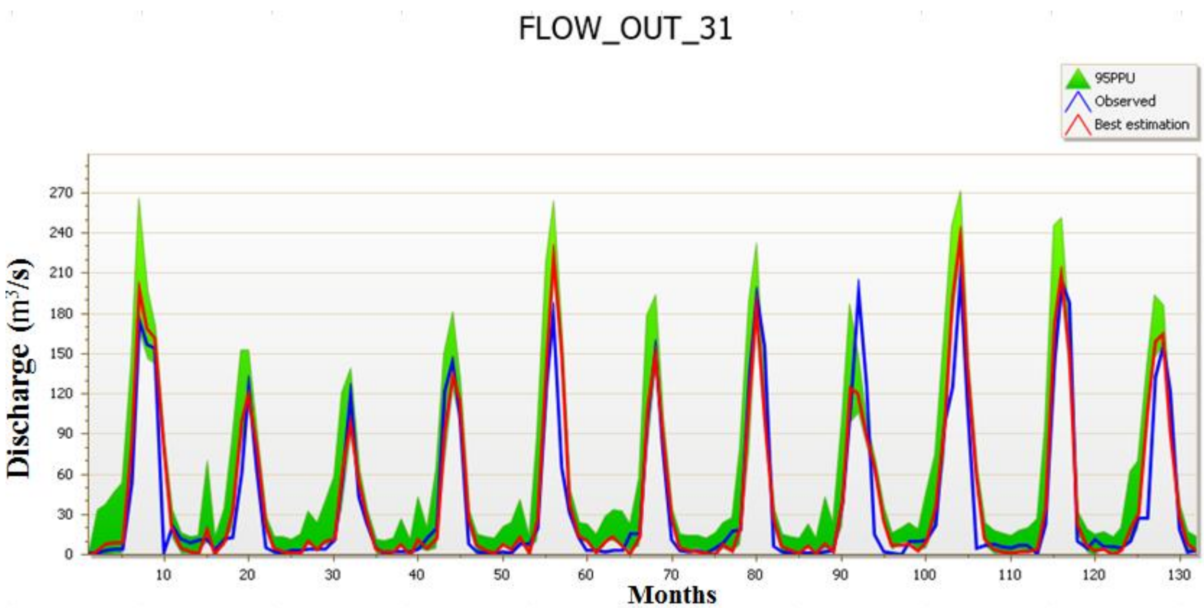

Figure 4-4 Hydrograph of the observed and simulated flow from the watershed for the calibration period monthly (2000-2010)

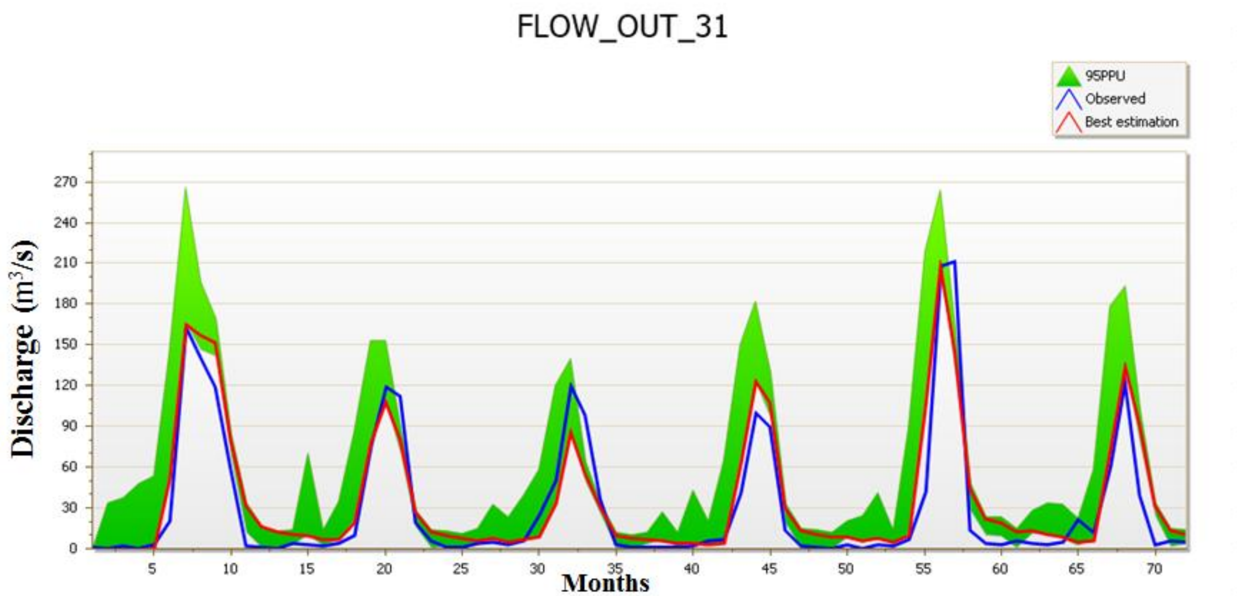

Figure 4.5 Hydrograph of the observed and simulated flow from the watershed for the validation period monthly (2011-2016).

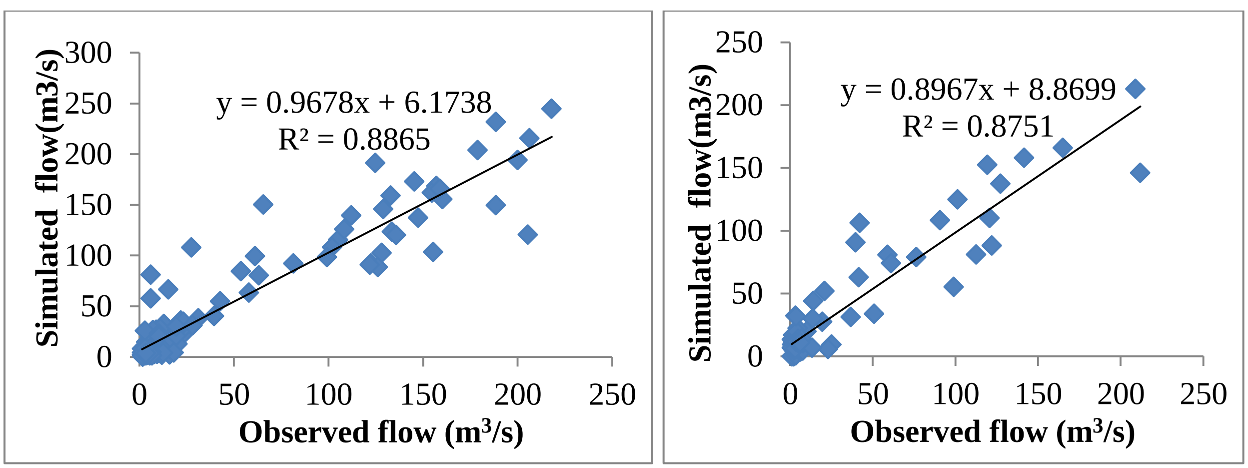

(A) (B)

Figure 4.6 Scatter diagram for simulated and observed flow during calibration (A) and validation (B)

4.3. Impact of Future Climate Change on streamflow

Changes in precipitation and minimum and maximum temperatures have an obvious effect on nature. As a result, the effect of climate change on streamflow was expected for this study based on seasonal and annual temperature and rainfall changes. The simulation results for the two scenarios for the future two-time horizons in terms of seasonal and annual percentage change relative to the base era.

The projected streamflow was simulated by using the SWAT model under RCP4.5 and RCP8.5 scenarios and presented by percentage changes concerning baseline streamflow. The predicted impact of climate change on streamflow on the Awash Bello sub-basin is based on the changes in temperature and precipitation projected under RCP 4.5 and RCP 8.5 scenarios. Thus, after calibrating the hydrological models with the observed record, the next step is the simulation of river flows in the sub-basin by using the bias-corrected precipitation, maximum and minimum temperature as input to hydrological models. Based on this, the streamflow impact of the Awash River was analyzed for two 30 years periods of baseline (2021-2050), 2050's and 2080s (2051-2080), and the hydrological model re-run for each case. SWAT simulation of the 1990-2019 period used as a base period against the future period of which the climate impact evaluated.

The seasonal change in percentage of simulated streamflow in m^3/s under both scenarios for the period of (2021-2050) and (2051-2080) has shown in figure 4.7 below. The result shows for the major rainy season, in the Kiremt (JJAS) major rainy season streamflow increases for all periods from the lowest +16.28% to the highest of +30.22% under both emission scenarios. The increment in streamflow can be seen in Belg (FMAM***)*** minor rainy season with +1.26% and +1.88% for a period of (2021-2050) under RCP4.5 and RCP8.5 emission scenarios respectively and for the period of (2051-2080) streamflow expected to reduce by -14.72% and -22.52% under RCP4.5 and RCP8.5 emission scenarios respectively. In the Bega (ONDJ) dry season, streamflow is expected to decrease within the range of (-16.95% to -33.12%) for all the periods under RCP4.5 and RCP8.5 emission scenarios. annual flow projected to increase by +4.22% and +2.71% for the period of (2021-2050) under RCP4.5 and RCP8.5 emission scenarios respectively. While for (2051-2080) annual streamflow is expected to decrease by -10.25% and -12.15% under RCP4.5 and RCP8.5 emission scenarios respectively. The finding of (Daba & You, 2020) shows that the projected annual streamflow increase in the middle-term and decrease in the far-term over the study area, ranging from -12.38% to 5.8% and the finding of (Getahun, 2018) shows the variation of streamflow is parallel to the variation of rainfall. This finding shows projected streamflow increase by 12% for the middle period in the sub-basin.

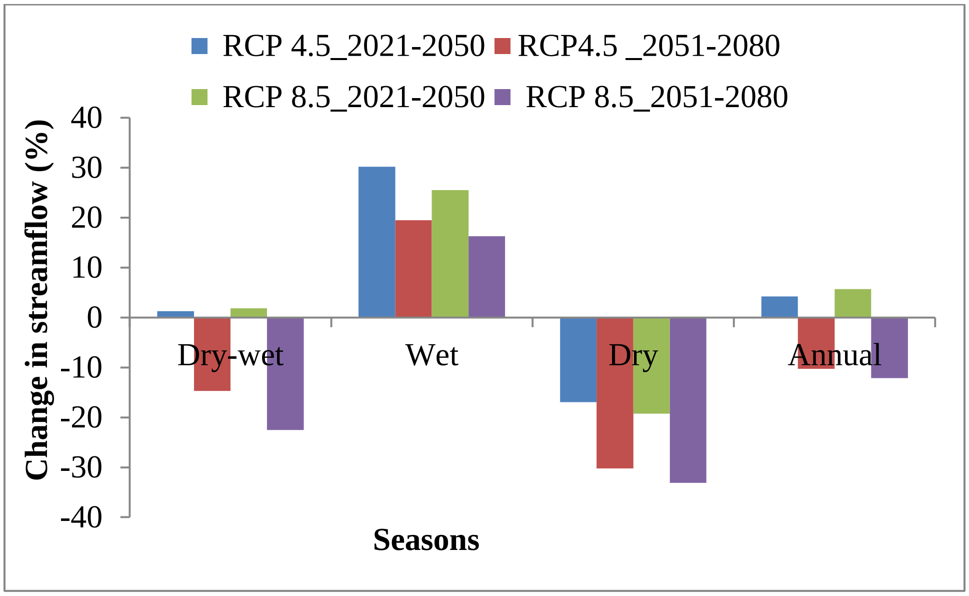

Figure 4.7 Annual and seasonal change under RCP4.5 and RCP8.5 for 2021-2050 and 2051-2080

5. CONCLUSION AND RECOMMENDATION

5.1 CONCLUSION

This study evaluates the impacts of climate change on the streamflow of Awash Bello sub-basin for the 2050s and 2080s under HadGEM2-ES for the two representative concentration pathways RCP 4.5 and RCP 8.5 climate scenario using SWAT hydrological model to simulate streamflow. Therefore, the future impact of climate change on hydro-meteorological characteristics of the awash Bello basin has been studied like: precipitation and Temperature for the 2050s (2021 - 2050) and 2080s (2051-5080) using data derived from downscaled climate data based on the coordinated regional climate downscaling experiment over African domain (CORDEX-Africa) with coupled Model Intercomparison project Phase5(CMIP5) simulations under representative concentration pathways RCP4.5 and RCP8.5 climate scenarios using SWAT2012 hydrological model.

The output RCM under different climate change scenarios (RCP4.5 and RCP8.5) and bias corrections of precipitation and temperature have been analyzed for current and two future time horizons (2021-2050 and 2051-2080) in the catchment.

The projection of precipitation and temperature changes showed differences in the two scenarios in both future periods. Under medium scenarios (RCP4.5), the annual precipitation of sub-basin will be increased by 4.85% and 7.56% in the 2050s (2021-2050) and decreased by -9.87% and -15.21% in 2080s (2051-2080) under intermediate (RCP4.5) and high (RCP8.5) emission scenario. The annual minimum temperature increased by up to 0.8^{o}c in the 2050s and 0.93^{o}c in the 2080s under the RCP4.5 scenario. On the other hand under RCP8.5, the annual minimum temperature increases by 1.06^{o}c and 1.38^{o}c in the 2050s and 2080's respectively.

The projected maximum temperature result shows that there will be an increase in maximum temperature in the middle-future and the far-future period for both scenarios. The annual maximum temperature for RCP 4.5 increased up to 1.06^{o}c and 1.28^{o}c in the 2050s and 2080s respectively. For RCP8.5, the annual maximum temperature will increase up to 1.13^{o}c and 1.43^{o}c in the 2050s and 2080s respectively.

The calibration and validation of the streamflow were made using SWAT-CUP with a method of SUFI2 in which for the calibration the period from 2000-2010 was taken and for the validation process, the period from 2011-2016 was taken. From the result, a good performance was found with R^2 and NSE greater than 0.6 and 0.5 respectively. The model performance criterion which is used to evaluate the model result indicates that the coefficient of determination (R^2) and Nash and Sutcliffe efficiency (NSE) are 0.89 and 0.87 for calibration and 0.88 and 0.86 for validation respectively. Following the calibration and validation, the SWAT model was rerun using the temperature and precipitation scenarios to predict the impact of climate changes on the streamflow of the river.

The sub-basin stream flow will have significant changes under predicted changes in precipitation and temperature. The change of streamflow, during the future period of 2021-2050 and 2051-2080 as compared to the baseline period 1990-2019. The annual streamflow in the 2050s increase by 4.22% and 2.71% under RCP4.5 and RCP8.5 scenarios. In the 2080s, annual streamflow under RCP4.5 and RCP8.5 scenarios was expected to decrease by -10.25% and -12.15% respectively. Generally, the results of this study are expected to arouse serious concern about water resource availability in the Awash Bello watershed under the warming climate.

5.2 RECOMMENDATION

As this study was done in a limited time and resource, the results should be taken as a starting point for further studies in the Awash Bello sub-basin on streamflow.

The result of this study is a basis for an informed decision in the water sector in terms of short and long-term implementation of development projects and also strategic planning policies. These results can also be used in the water sector for water resources management and policymakers.

According to the study, the following major recommendations are suggested:

- In this study, the analysis of climate change impact has been done by evaluating its primary appearance of changes in precipitation and temperature data under two scenarios and evaluated by assuming that the land cover will remain the same for the historic as well as for future periods. The study also does not consider any change in soil parameters at future time horizons. However, in the real world, the land cover change and soil parameters will occur due to natural and human influences. so, it is more appreciable when considering the change in land use, soil, and other climate variables such as (relative humidity, wind speed, etc.) as inputs in addition to the change in precipitation and temperature for a better understanding of the climate change impact on the catchment.
- There are problems in the Awash Bello sub-basin especially on streamflow which is highly decreasing. Therefore, further research is recommended in the Awash Bello sub-basin.
- The meteorological and hydrological data have a significant effect on the outcome of impact studies. Therefore, as much as possible it should take long years to record data with accuracy and quality. The researcher should be concerned about this matter and all people concerned should pay special attention to data management and reliable data recording.

REFERENCE

Aawar, T., & Khare, D. (2020). Assessment of climate change impacts on streamflow through the hydrological model using SWAT model : a case study of Afghanistan. Modeling Earth Systems and Environment, 0123456789. https://doi.org/10.1007/s40808-020-00759-0

Abbasa, N., Wasimia, S. A., & Al-ansari, N. (2016). Assessment of Climate Change Impacts on Water Resources of Al-Adhaim, Iraq Using SWAT Model. 716–732. https://doi.org/10.4236/eng.2016.810065

Abbaspour, K. . (2015). SWAT-CUP: SWAT Calibration and Uncertainty Programs - A User Manual. Swiss Federal Institute Science and Technology, Eawag: Duebendorf, Switzerland. https://doi.org/10.1007/s00402-009-1032-4

Abbaspour, K. C., Rouholah Nejad, E., Vaghefi, S., Srinivasan, R., Yang, H., & Kløve, B. (2015). A continental-scale hydrology and water quality model for Europe: Calibration and uncertainty of a high-resolution large-scale SWAT model. Journal of Hydrology, 524, 733–752. https://doi.org/10.1016/j.jhydrol.2015.03.027

Abera, F. F. (2011). Assessment of Climate Change Impacts on the Hydrology of Upper Guder Catchment, Upper Blue Nile. https://pdfs.semanticscholar.org.pdf

Abiodun, B. J., & Adedoyin, A. (2016). Chapter 23 - A Modelling Perspective of Future Climate Change. In Climate Change (Second Edi). Elsevier B.V. https://doi.org/10.1016/B978-0-444-63524-2.00023-3

Agency, U. S. E. P. (2021). overview-greenhouse-gases.

Agency, U. state environmental protection. (2017). causes-climate-change_.

Akpoti, K. (2016a). Impact of Rainfall Variability, Land Use and Land Cover Change on Stream Flow for Hydropower Generation in the Black Volta Basin. Hydrology, 3(3), 26. https://doi.org/10.13140/RG.2.2.15869.67040

Akpoti, K. (2016b). Impact of Rainfall Variability, Land Use and Land Cover Change on Stream Flow for Hydropower Generation in the Black Volta Basin. Hydrology, 3(3), 26.

https://doi.org/10.13140/RG.2.2.15869.67040

Akpoti, K., Antwi, E. O., & Kabo-bah, A. T. (2016). Impacts of rainfall variability, land use, and land cover change on streamflow of the Black Volta basin, West Africa. Hydrology, 3(3), 1–24. https://doi.org/10.3390/hydrology3030026

Alemayehu, T. (2017). Stream Flow and Sediment Yield : A Case Study of Upper Awash Basin.

Amin, A., & Nuru, N. (2020). Evaluation of the Performance of SWAT Model to Simulate Stream Flow of Mojo River Watershed: In the Upper Awash River Basin, in Ethiopia. Hydrology, 8(1), 7. https://doi.org/10.11648/j.hyd.20200801.12

Angelo, M. J., & Du Plessis, A. (2017). Research handbook on climate change and agricultural law. Research Handbook on Climate Change and Agricultural Law, 1–472. https://doi.org/10.4337/9781784710644

Arnold, J. G., Allen, P. M., Volk, M., Williams, J. R., & Bosch, D. D. (2010). Assessment Of Different Representations of Spatial Variability on Swat Model Performance. 53(5), 1433–1443.

Ayele, G. T., Teshale, E. Z., Yu, B., Rutherfurd, I. D., & Jeong, J. (2017). Streamflow and sediment yield prediction for watershed prioritization in the upper Blue Nile river basin, Ethiopia. Water (Switzerland), 9(10). https://doi.org/10.3390/w9100782

Bekele, D., Alamirew, T., Kebede, A., Zeleke, G., & Melesse, A. M. (2019). Modeling Climate Change Impact on the Hydrology of Keleta Watershed in the Awash River Basin, Ethiopia. 95–107.

Bjornaes, C., & Ni, E. (2015). A guide to Representative Concentration Pathways.

Bokke, A. S., Taye, M. T., Willems, P., & Siyoum, S. A. (2017). Validation of General Climate Models (GCMs) over Upper Blue Nile River Basin, Ethiopia. Atmospheric and Climate Sciences, 07(01), 65–75. https://doi.org/10.4236/acs.2017.71006

Cambien, N., Gobeyn, S., Nolivos, I., Eurie Forio, M. A., Arias-Hidalgo, M., Dominguez-Granda, L., Witing, F., Volk, M., & Goethals, P. L. M. (2020). Using the soil and water assessment tool to simulate the pesticide dynamics in the data-scarce guayas River Basin, Ecuador. Water (Switzerland), 12(3), 1–21. https://doi.org/10.3390/w12030696

Canada, G. of. (2019). Causes of climate change.

Chandra, R., Basnet, K., & Sherchan, B. (2019). Application of HEC-HMS Model for Runoff Simulation : A Case Study of Marshyangdi River Basin in Nepal. December, 127–140.

Cryosphere, T., Cryosphere, T., Barth, S., & Earth, S. (2013). Influence of downscaling methods in projecting climate change impact on hydrological extremes of upper Blue Nile basin. https://doi.org/10.5194/hessd-10-7857-2013

Cunderlik, J. (2003). Hydrological model selection for the CFCAS project: assessment of water resources risk and vulnerability to changing climate condition.

Daba, M. H., & You, S. (2020). Assessment of climate change impacts on river flow regimes in the upstream of the awash basin, Ethiopia: Based on IPCC fifth assessment report (ar5) climate change scenarios. Hydrology, 7(4), 1–22. https://doi.org/10.3390/hydrology7040098

Daba, T. (2017). Sediment Problem of Gefersa Reservoirs and The Appropriate Mitigation. MSc Thesis, Addis Ababa University. 3412.

Demissie, T. A., Saathoff, F., Sileshi, Y., & Gebissa, A. (2013). Climate change impacts on the streamflow and simulated sediment flux to Gilgel Gibe 1 hydropower reservoir – Ethiopia. 2(2), 63–77.

Desta, A. G. (2017). Evaluation of The Impacts of Climate Change on Water Resources of Omo-Gibe River Basin (Case study of Gibe III catchment).

Dibaba, W. T., Demissie, T. A., & Miegel, K. (2020). Watershed hydrological response to combined land use/land cover and climate change in highland Ethiopia: Finchaa catchment. Water (Switzerland), 12(6). https://doi.org/10.3390/w12061801

Dibaba, Wakjira T., Miegel, K., & Demissie, T. A. (2019). Evaluation of the CORDEX regional climate models performance in simulating climate conditions of two catchments in Upper

Blue Nile Basin. *Dynamics of Atmospheres and Oceans*, *87*(August), 101104. https://doi.org/10.1016/j.dynatmoce.2019.101104

Dierickx, F. (2019). Copernicus Climate Change Programme: User Learning Service Content.

Dile, Y. T., Berndtsson, R., & Setegn, S. G. (2013). Hydrological Response to Climate Change for Gilgel Abay River, in the Lake Tana Basin - Upper Blue Nile Basin of Ethiopia. 8(10), 12–17. https://doi.org/10.1371/journal.pone.0079296

Doktor-ingenieur, G., Universit, U., & Mohammed, A. K. (2013). The Effect of Climate Change on Water Resources Potential of Omo Gibe Basin , Ethiopia Dissertation Fakultät für Bauingenieurwesen und Umweltwissenschaften Universität der Bundeswehr München vorgelegt von.

Elbehri, A. (2015). Climate Change and Global assessments and implications for food security and trade.

Gashaw, T., Tulu, T., Argaw, M., & Worqlul, A. W. (2018). Science of the Total Environment Modeling the hydrological impacts of land use/land cover changes in the Andassa watershed, Blue Nile Basin, Ethiopia. Science of the Total Environment, 619–620, 1394–1408. https://doi.org/10.1016/j.scitotenv.2017.11.191

Gebre, S. L. (2015). Application of the HEC-HMS Model for Runoff Simulation of Upper Blue Nile River Basin. Journal of Waste Water Treatment & Analysis, 06(02). https://doi.org/10.4172/2157-7587.1000199

Gebrie, T., Engineering, W. R., Tabor, D., & Jemberie, M. (2016). Sediment Yield Modeling of Dedissa Sub Basin, Abay Basin, 6(10), 120–127.

Geremew, A. A. (2013). Assessing The Impacts of Land Use and Land Cover Change on Hydrology of Watershed : A Case study on Gilgel – Abbay Watershed, Lake Tana. 82.

Gessesse, A. A., Melesse, A. M., Abera, F. F., & Abiy, A. Z. (2019). Modeling Hydrological Responses to Land Use Dynamics, Choke, Ethiopia. Water Conservation Science and Engineering, 4(4), 201–212. https://doi.org/10.1007/s41101-019-00076-3

Getahun, Yitea, S. M.-H. L. P.-Y. C. (2020). Assessing Impact of Climate Change on Hydrology of Melka Kuntrie Subbasin, Ethiopia with Ar4 and Ar5 Projections.

Getahun, Y. S. (2018). Impact of Climate Change on Hydrology of the Upper Awash River Basin (Ethiopia): Inter-comparison of old SRES and new RCP scenarios. April 2015.

Gharbia, S. S., Gill, L., Johnston, P., & Pilla, F. (2016). Multi-GCM ensembles performance for climate projection on a GIS platform. Modeling Earth Systems and Environment, 2(2), 1–21. https://doi.org/10.1007/s40808-016-0154-2

Ghimire, U., Akhtar, T., Shrestha, N., & Daggupati, P. (2019). Development of Asia Pacific Weather Statistics (APWS) dataset for use in Soil and Water Assessment Tool (SWAT) simulation. Earth System Science Data Discussions, November, 1–30. https://doi.org/10.5194/essd-2019-178

Giorgi, F., & Gutowski, W. J. (2015). Regional Dynamical Downscaling and the CORDEX Initiative. Annual Review of Environment and Resources, 40, 467–490. https://doi.org/10.1146/annurev-environ-102014-021217

Gizaw, M. S., Biftu, G. F., Gan, T. Y., Moges, S. A., & Koivusalo, H. (2017). The potential impact of climate change on streamflow of major Ethiopian rivers. Climatic Change, 143(3–4), 371–383. https://doi.org/10.1007/s10584-017-2021-1

Group, C. A., Central, C., & Livermore, L. (2013). Downscaled CMIP3 and CMIP5 Climate Projections. May.

Guntukula, R. (2019). Assessing the impact of climate change on Indian agriculture : Evidence from major crop yields. September, 1–7. https://doi.org/10.1002/pa.2040

Haile, A. T., & Rientjes, T. (2015). SC. Atmospheric Research. https://doi.org/10.1016/j.atmosres.2015.03.013

Hailemariam, K. (1999). Impact of climate change on the water resources of Awash River Basin, Ethiopia. Climate Research, 12(2-3 SPEC. ISS. 6), 91–96. https://doi.org/10.3354/cr012091

Hakala, K. (2020). Hydrological Modeling of Climate Change Impacts Hydrological Modeling of Climate Change Impacts. February. https://doi.org/10.1002/9781119300762.wsts0062

Hayhoe, K., Edmonds, J., Kopp, R. E., LeGrande, A. N., Sanderson, B. M., Wehner, M. F., & Wuebbles, .J. (2017). Climate Models, Scenarios, and Projections. Climate Science Special Report: Fourth National Climate Assessment, I, 133–160. https://doi.org/10.7930/J0WH2N54.U.S.

Her, Y., Frankenberger, J., & Chaubey, I. (2015). Threshold Effects in HRU Definition of the Soil and Water Assessment Tool. April. https://doi.org/10.13031/trans.58.10805

IPCC. (2013). IPCC Climate Change 2013 Climate Change 2013. In Researchgate.Net. https://doi.org/10.1017/CBO9781107415324.Summary

J.G. Arnold, D. N. Moriasi, P. W. Gassman, K. C. Abbaspour, M. J. White, R. Srinivasan, C. Santhi, R. D. Harmel, A. van Griensven, M. W. Van Liew, N. Kannan, M. K. J. (2012). Swat: Model Use, Calibration, And Validation. 55(4), 1491–1508.

Jilo, N. B. (2019). Evaluation of the Impacts of Climate Change on Sediment Yield from the Logiya Watershed, Lower. Hydrology.

Jones, C. D., Hughes, J. K., Bellouin, N., Hardiman, S. C., Jones, G. S., Knight, J., Liddicoat, S., Connor, F. M. O., & Laplace, I. P. (2011). Model Development The HadGEM2-ES implementation of CMIP5 centennial simulations. 543–570. https://doi.org/10.5194/gmd-4-543-2011

Kalcic, M. M., Chaubey, I., & Frankenberger, J. (2015). Defining Soil and Water Assessment Tool (SWAT) hydrologic response units (HRUs) by field boundaries. 8(3), 69–80. https://doi.org/10.3965/j.ijabe.20150803.951

Kangume, C., & Mulungu, D. M. M. (2018). Assessing the Impacts of Climate Change on Streamflow in Malaba River Catchment, Uganda. SSRN Electronic Journal, January. https://doi.org/10.2139/ssrn.3210592

Kazi, R., & Mohamed, M. Hantush, Alexander, Hall, and J. M. (2019). Report Watershed Hydrologic and Contaminated Sediment Transport Modeling in the Tri-State Mining

District Watershed Hydrologic and Contaminated Sediment Transport Modeling in the Tri-State Mining District.

Kefeni, K., Mokonnen, B., & Roba, N. (2020). Evaluation of the Performance of Regional Climate Models in Simulating Rainfall Characteristics over Upper Awash Sub-Basin, Ethiopia. 5(1), 134–138.

KIFLE, T. (2020). Hydrological Modeling of Climate Change Impacts in Awash River Basin : A Case of Borkena River Catchment, Ethiopia.

Legesse Gebre, S. (2015). Hydrological Response to Climate Change of the Upper Blue Nile River Basin: Based on IPCC Fifth Assessment Report (AR5). Journal of Climatology & Weather Forecasting, 03(01), 1–15. https://doi.org/10.4172/2332-2594.1000121

Lemma, M. (2018). Sediment Yield Modeling Using Swat, Case StudyoOf Upper Awash Basin Ethiopia

Leng, M., Yu, Y., Wang, S., & Zhang, Z. (2020). Simulating the Hydrological Processes of a. Water.

Leta, M. K. (2017). Sediment Yield Assessment and Mitigation Measures in Finchaa Watershed, Ethiopia. 6(08), 220–227.

Malhi, G. S., Kaur, M., & Kaushik, P. (2021). Impact Of Climate Change On Agriculture And Its Mitigation Strategies: A Review. Sustainability (Switzerland), 13(3), 1–21. Https://Doi.Org/10.3390/Su13031318

Mammo, D. A. (2017). Impact of Climate Change on Hydrological Behavior of Ankara Watershed, Northern Awash Basin, Ethiopia. 4(August), 9–15.

Megersa, T., Nedaw, D., & Argaw, M. (2019). The combined effect of land use/cover types and slope gradient in sediment and nutrient losses in Chancho and Sorga sub-watersheds, East Wollega Zone, Oromia, Ethiopia. Environmental Systems Research, 8(1). https://doi.org/10.1186/s40068-019-0151-3

Mohammed, A. K., 2013. (2013). The Effect of Climate Change on Water Resources Potential of

Omo Gibe Basin, Ethiopia. PhD Dissertation, Universität Der Bundeswehr, München, Germany., 10(2), 915–924.

Muleta, T. N. (2021). Climate change scenario analysis for Baro - Akobo river basin, Southwestern Ethiopia. Environmental Systems Research. https://doi.org/10.1186/s40068-021-00225-5

Namara,Wana Geyisa, D. I. T. A. D. and F. G. T. (2020). Rainfall-Runoff Modeling Using Hec-Hms: The Case of Awash Bello Sub-Catchment, Upper Awash Basin, Ethiopia Wana. International Journal of Environment, 1(1), 9–19.

Nasiri, S., Ansari, H., & Ziaei, A. N. (2020). Simulation of water balance equation components using SWAT model in Samalqan Watershed (Iran). Arabian Journal of Geosciences, 13(11). https://doi.org/10.1007/s12517-020-05366-y

NMA. (2007). Climate Change National Adaptation Programs of Action (Napa) Of Ethiopia Editor: Water (Switzerland), 2(June), 73pp. https://doi.org/10.1016/j.cliser.2019.

Obasi, A. A., Ogbu, K. N., Ndulue, E. L., Ogwo, V. N., & Mbajiorgu, C. C. (2018). Prediction of the impacts of climate changes on the streamflow of Ajali River Watershed using SWAT model. Nigerian Journal of Technology, 36(4), 1286. https://doi.org/10.4314/njt.v36i4.39

Pachauri, R. K. (2014). Climate Change 2014 Synthesis Report.

Pachauri, R. K., Reisinger, A., Bernstein, L., Bosch, P., Canziani, O., Chen, Z., Christ, R., Davidson, O., Hare, W., Huq, S., Karoly, D., Kattsov, V., Kundzewicz, Z., Liu, J., Manning, M., Matsuno, T., Menne, B., Metz, B., Mirza, M., … Yohe, G. (2007). Climate Change 2007.

Policymakers, S. (2018). Summary for Policymakers.

Raes, D., Willems, P. and GBaguidi, F. (2006). RAINBOW - a software package for hydrometeorological frequency analysis and testing the homogeneity of historical data sets. January, 27–31.

Reay, D., Sabine, C., Smith, P., & Hymus, G. (2007). Intergovernmental Panel on Climate

Change. Fourth Assessment Report. Geneva, Switzerland: Intergovernmental Panel on Climate Change. Cambridge; UK: Cambridge University Press; 2007. Available from: www. ipcc.ch. In Intergovernmental Panel on Climate Change. https://doi.org/10.1038/446727a

Roth, V., Lemann, T., Zeleke, G., Subhatu, A. T., Nigussie, T. K., & Hurni, H. (2018). Effects of climate change on water resources in the upper Blue Nile Basin of Ethiopia. Heliyon, 4(9). https://doi.org/10.1016/j.heliyon.2018.e00771

Sab-basin, U. A., & Daba, M. H. (2018). Sensitivity of SWAT Simulated Runoff to Temperature and Rainfall in the. 9(1), 1–7. https://doi.org/10.4172/2157-7587.1000293

Santhi, C., Arnold, J. G., Williams, J. R., Dugas, W. A., Srinivasan, R., & Hauck, L. M. (2001). Validation of the SWAT model on a large river basin with point and nonpoint sources. Journal of the American Water Resources Association, 37(5), 1169–1188. https://doi.org/10.1111/j.1752-1688.2001.tb03630.x

Sci, J. E., Chang, C., & Ky, R. (2014a). Earth Science & Climatic Change Impact of Climate Change on Water Resources. 5(3). https://doi.org/10.4172/2157-7617.1000185

Sci, J. E., Chang, C., & Ky, R. (2014b). Impact of Climate Change on Water Resources. Journal of Earth Science & Climatic Change, 05(03). https://doi.org/10.4172/2157-7617.1000185

Setegn, S. G., Rayner, D., Melesse, A. M., Dargahi, B., & Srinivasan, R. (2011). Impact of climate change on the hydro-climatology of Lake Tana Basin, Ethiopia. Water Resources Research, 47(4), 1–13. https://doi.org/10.1029/2010WR009248

Shimelash Molla. (2017). Assessment of Climate Change Impact on streamflow of Baro-Akobo River Basin Case study of Baro Catchment.

Sime, C. H., Demissie, T. A., & Tufa, F. G. (2020). Surface runoff modeling in Ketar watershed, Ethiopia. Journal of Sedimentary Environments, 5(1), 151–162. https://doi.org/10.1007/s43217-020-00009-4

Steve, D. (2020). Scientific assessments of climate change in northern regions. February.

Stocker, T. F., Allen, S. K., Bex, V., & Midgley, P. M. (2013). Climate Change 2013 The Physical Science Basis Working Group I Contribution to the Fifth Assessment Report of the Intergovernmental Panel on Climate Change Edited by.

subarmaniya.pdf. (2008).

T. Lenhart *, K. Eckhardt, N. Fohrer, H.-G. F. (2002). Comparison of two different approaches of sensitivity analysis. Physics and Chemistry of the Earth, 3(3), 645–654. https://doi.org/10.1007/BF01743071

T.T. DERESSA, R. M. H. A. N. D. C. R. (2011). Perception of and adaptation to climate change by farmers in the Nile basin of Ethiopia. 2011, 23–31. https://doi.org/10.1017/S0021859610000687

Tadese, M. T., Kumar, L., Koech, R., & Zemadim, B. (2019). Hydro-climatic variability: A characterization and trend study of the Awash River Basin, Ethiopia. Hydrology, 6(2). https://doi.org/10.3390/hydrology6020035

Tariku, T. B., Gan, T. Y., Li, J., & Qin, X. (2021). Impact of Climate Change on Hydrology and Hydrologic Extremes of Upper Blue Nile River Basin. Journal of Water Resources Planning and Management, 147(2), 04020104. https://doi.org/10.1061/(asce)wr.1943-5452.0001321

Taye, M. T., Dyer, E., Hirpa, F. A., & Charles, K. (2018). Climate change impact on water resources in the Awash basin, Ethiopia. Water (Switzerland), 10(11), 1–16. https://doi.org/10.3390/w10111560

Taylor, K. E., Stouffer, R. J., & Meehl, G. A. (2012). An overview of CMIP5 and the experiment design. Bulletin of the American Meteorological Society, 93(4), 485–498. https://doi.org/10.1175/BAMS-D-11-00094.1

Teutschbein, C. (2013). Hydrological Modeling for Climate Change Impact Assessment: Transferring Large-Scale Information from Global Climate Models to the Catchment Scale. In Department of Physical Geography and Quaternary Geology: Vol. Ph.D.

Thavhana, M. P., Savage, M. J., & Moeletsi, M. E. (2018). SWAT model uncertainty analysis, calibration, and validation for runoff simulation in the Luvuvhu River catchment, South Africa. Physics and Chemistry of the Earth, 105, 115–124. https://doi.org/10.1016/j.pce.2018.03.012

Tigabu, T. B., Wagner, P. D., Hörmann, G., Kiesel, J., & Fohrer, N. (2020). Climate change impacts the water and groundwater resources of the Lake Tana Basin, Ethiopia. Journal of Water and Climate Change, 1–20. https://doi.org/10.2166/wcc.2020.126

Todd, M. C., Thompson, J. R., Taylor, R. G., Nay, A. E., & Ayenew, T. (2020). Uncertainty assessment in river flow projections for Ethiopia's Upper Awash Basin using multiple GCMs and hydrological models. Hydrological Sciences Journal, 0(0), 1. https://doi.org/10.1080/02626667.2020.1767782

Tufa, F. G., & Sime, C. H. (2020). Streamflow modeling using SWAT model and the model performance evaluation in Toba sub-watershed, Ethiopia. Modeling Earth Systems and Environment, 0123456789. https://doi.org/10.1007/s40808-020-01039-7

van Vuuren, D. P., Edmonds, J., Kainuma, M., Riahi, K., Thomson, A., Hibbard, K., Hurtt, G. C., Kram, T., Krey, V., Lamarque, J. F., Masui, T., Meinshausen, M., Nakicenovic, N., Smith, S. J., & Rose, S. K. (2011). The representative concentration pathways: An overview. Climatic Change, 109(1), 5–31. https://doi.org/10.1007/s10584-011-0148-z

Vedula, S., & Mujumdar, P. P. (2005). Water Resources Systems: Modelling Techniques and Analysis. Water Resources Systems, October, 279.

Weregna, M. (2019). Rainfall-Runoff Modeling Using SWAT Hydrologic Model: Case Study of DabusRiver Watershed, Ethiopia.

Yimer, A. (2018). Evaluation of climate change impact on streamflow of Mille watershed.

APPENDIX

Appendix A: Hydro-Meteorological data

Table A-1 Yearly sum RF (mm) of stations

year	Addis Alem	Ginchi	Ambo	Teji	Tullubolo
1990	1603.4	1149.8	1120	990.8	781.3
1991	627.528	1444.9	1022.3	961	782.2904
1992	717.288	1292.2	1044	962	1656.1
1993	714.56	1417.4	1157.8	1093.6	2258.2
1994	1160.08	1486.4	1043.8	866.1	1375.7
1995	1260.5	1125.6	1072.5	786.8	566.6601
1996	1270.644	905.1	811.5	946.1	1217.4
1997	1371.076	1023.6	781	794.7	1171.7
1998	1473.7	1463	841.7	1135.7	1448.2
1999	1435.124	1173.5	821.6	833.8	1372.4
2000	625.744	999.4	904.1	866.1	1215.5
2001	1182.7	1242.2	1079.5	872.5	821.4
2002	800.7	1029.2	769.4	811.1	1021.5
2003	947.4	1226.5	932.2	1082	979.4
2004	1094.984	1035.5	944	941.9	1158.6
2005	2189.728	993.2	856.6	1112.6	1124.3
2006	1211.396	1102.6	1103.9	1170.9	1039
2007	1342.3	1047.4	1163.1	969.3	1161.9
2008	620.1	1082.8	1160.3	806.5	1139.1
2009	1386.652	1133.3	1006.4	809.6	978.7
2010	956.075	1148.3	1187.6	1408.799	1394.8
2011	990.348	2152.6	1885.1	902.5	853.7
2012	352.544	1090.7	956.1	717.6908	919.6
2013	413.104	1035.489	960	965.4	1683.6
2014	418.968	820.736	866.1	844.8	1019.2
2015	773.8	839.709	950.2	835.1	852.7
2016	1040.33	1091.3	915.6	1197.418	947.6
2017	601	1178.1	815	722.1918	1206.7
2018	1170.4	1169	1280.7	845.3	1218.8
2019	1098.4	1418.1	1145.9	1017.5	1070.1

Table A-2 Observed areal mean monthly precipitation (mm) over the study

Month	Areal Precipitation
January	565.448
February	678.511
March	1639.679
April	2280.799
May	2699.797
June	5797.938
July	8630.756
August	8072.725
September	4397.092
October	1228.162
November	427.227
December	283.599

Table A-3 Yearly maximum temperature (^{o}c)

Year	**Addis Alem**	**Teji**	**Tefki**	**Tulu bolo**	**Ginchi**
1990	24.14	22.60	27.09	23.13	24.14
1991	24.11	22.94	27.07	26.01	24.11
1992	23.95	23.35	27.01	27.08	23.95
1993	23.87	23.22	26.96	27.43	23.87
1994	24.02	22.61	26.98	26.94	24.02
1995	24.04	22.82	26.98	23.89	24.04
1996	24.11	23.19	27.06	21.93	24.11
1997	23.07	22.82	26.93	22.05	23.07
1998	23.81	22.63	26.92	21.44	23.81
1999	23.48	23.42	27.02	21.27	23.48
2000	23.76	23.70	26.92	21.19	23.76
2001	23.76	23.43	26.95	25.30	23.76
2002	24.72	24.09	26.92	25.73	24.72
2003	24.49	23.77	26.95	25.40	24.49
2004	24.56	23.97	26.92	26.36	24.56
2005	24.37	23.73	26.88	26.22	24.37
2006	24.02	23.66	27.04	25.72	24.02
2007	23.89	22.93	26.96	25.57	23.89
2008	23.64	22.80	26.96	25.64	23.64
2009	24.37	22.91	26.98	25.51	24.37
2010	24.09	23.29	26.11	25.58	24.09
2011	25.06	22.59	26.69	25.58	25.06

2012	23.70	22.94	27.29	25.44	23.70
2013	24.93	23.20	27.07	25.43	24.93
2014	25.04	23.27	27.00	25.51	25.04
2015	24.95	23.31	27.87	25.54	24.95
2016	25.88	28.30	28.30	25.51	25.88
2017	24.04	28.67	28.66	25.72	24.04
2018	27.04	26.86	27.85	25.51	27.04
2019	23.78	27.81	27.81	25.53	23.78

Table A-4 yearly minimum temperature (^{o}c)

Year	**Addis Alem**	**Teji**	**Tefki**	**Tulu bolo**	**Ginchi**
1990	9.34	9.60	8.45	6.48	12.00
1991	9.37	9.86	8.45	6.34	11.46
1992	9.38	11.04	8.36	10.60	11.45
1993	9.14	11.07	8.31	10.78	11.56
1994	9.17	10.64	8.48	11.48	12.00
1995	9.56	10.63	8.37	12.94	11.71
1996	9.54	11.25	8.37	12.56	10.73
1997	9.54	10.98	8.48	12.49	11.68
1998	10.11	10.59	8.32	11.63	11.63
1999	8.76	10.20	8.25	10.47	11.67
2000	7.96	10.64	8.47	9.80	11.65
2001	7.77	10.46	8.34	11.06	11.33
2002	8.23	10.65	8.34	11.33	11.45
2003	10.52	11.11	8.38	11.25	11.42
2004	12.36	10.12	8.34	10.67	11.43
2005	11.61	10.59	8.32	10.75	11.64
2006	9.88	10.30	8.42	10.57	10.76
2007	9.62	11.05	8.44	11.66	11.59
2008	9.36	11.26	8.30	11.53	11.52
2009	9.68	11.49	8.39	11.08	11.52
2010	9.72	10.47	10.73	11.69	11.58
2011	9.77	9.60	10.09	10.92	11.62
2012	9.33	9.86	10.10	10.61	11.62
2013	9.34	10.59	10.33	10.88	11.57
2014	9.24	10.55	10.92	10.82	11.60
2015	8.66	10.52	10.46	10.47	11.61
2016	9.83	11.00	10.96	11.11	11.62
2017	8.87	9.75	9.69	10.29	11.48
2018	10.38	10.89	10.88	10.65	11.60

2019	10.97	10.35	10.31	10.40	11.61

Table A-5 Mean monthly areal Temperature (^{o}c)

Month	Areal TMAX	Areal TMIN
JAN	25.55	10.04
FEB	25.89	11.52
MAR	25.00	11.03
APR	25.96	11.19
MAY	26.12	11.29
JUN	25.02	10.78
JUL	23.80	10.58
AUG	23.82	10.61
SEP	24.31	10.48
OCT	24.90	10.10
NOV	25.20	10.76
DEC	25.05	10.67

Appendix B: Homogeneity of awash Bello stations

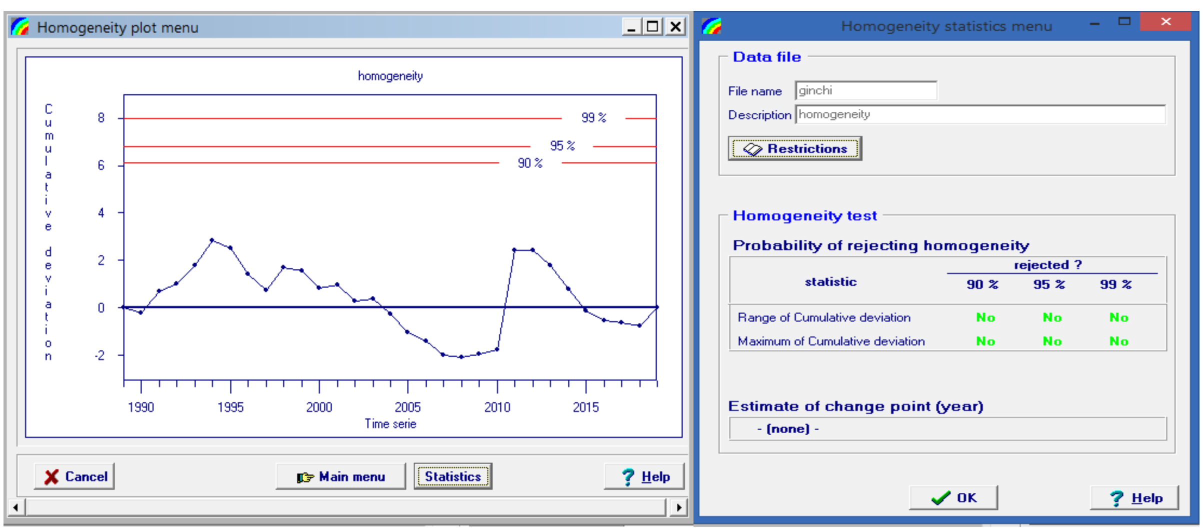

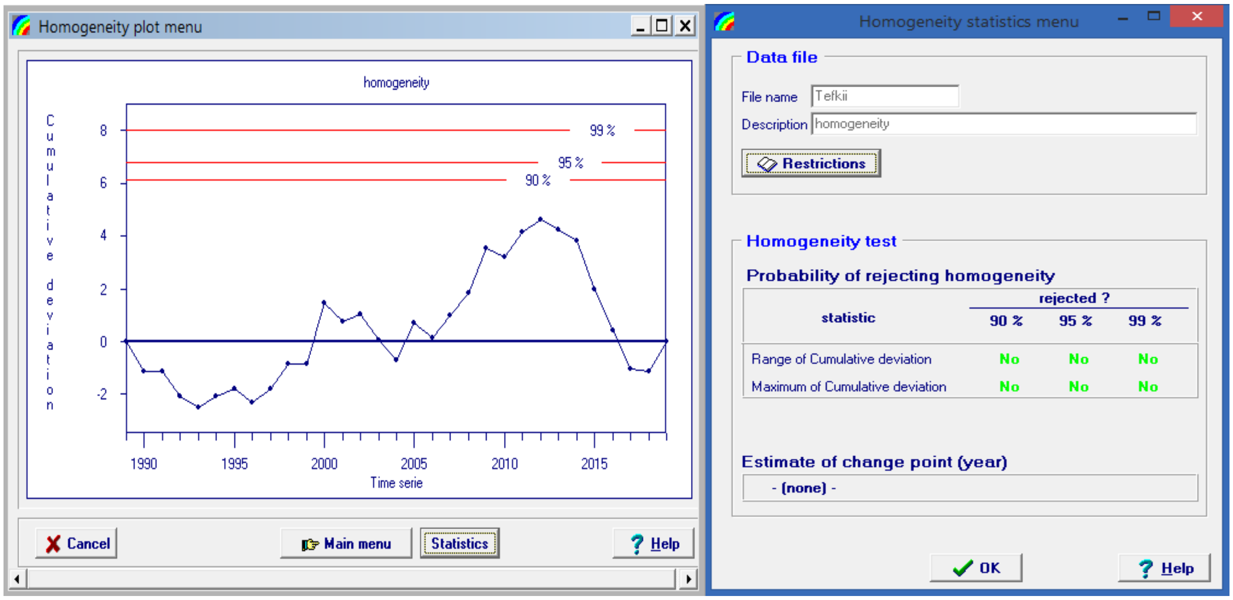
Homogeneity plot menu
homogeneity
Cumulative deviation
99 %
95 %
90 %
1990
1995
2000
2005
2010
2015
Time serie
Cancel
Main menu
Statistics
Help
Homogeneity statistics menu
Data file
File name Tefkii
Description homogeneity
Restrictions
Homogeneity test
Probability of rejecting homogeneity
statistic
rejected ?
90 % 95 % 99 %
Range of Cumulative deviation No No No
Maximum of Cumulative deviation No No No
Estimate of change point (year)
- (none) -
OK
Help

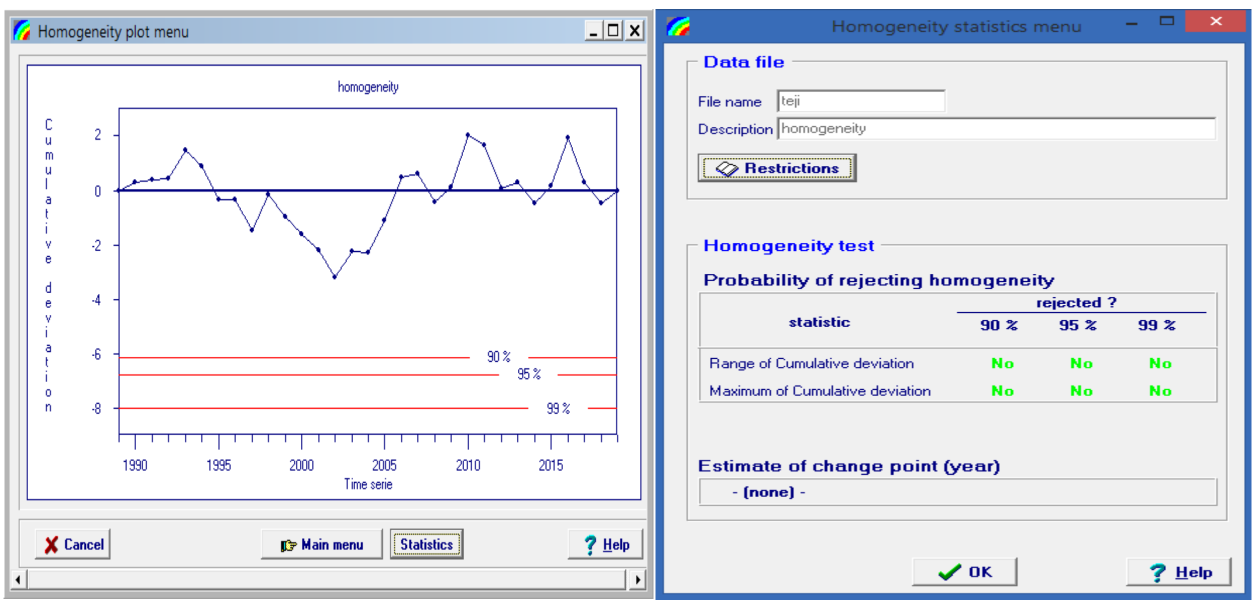
Homogeneity plot menu
homogeneity
Cumulative deviation
90 %
95 %
99 %
1990
1995
2000
2005
2010
2015
Time serie
Cancel
Main menu
Statistics
Help
Homogeneity statistics menu
Data file
File name teji
Description homogeneity
Restrictions
Homogeneity test
Probability of rejecting homogeneity
statistic
rejected ?
90 % 95 % 99 %
Range of Cumulative deviation No No No
Maximum of Cumulative deviation No No No
Estimate of change point (year)
- (none) -
OK
Help

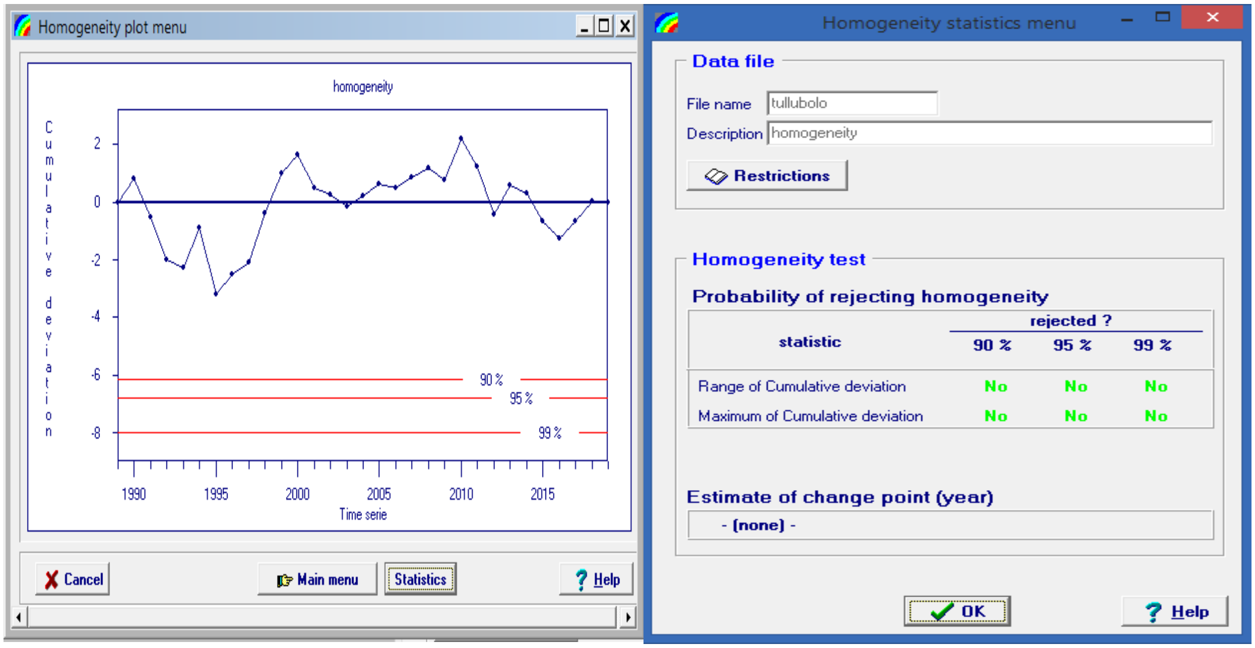

Appendix c: Land use /cover Soil types of Awash Bello sub-basin

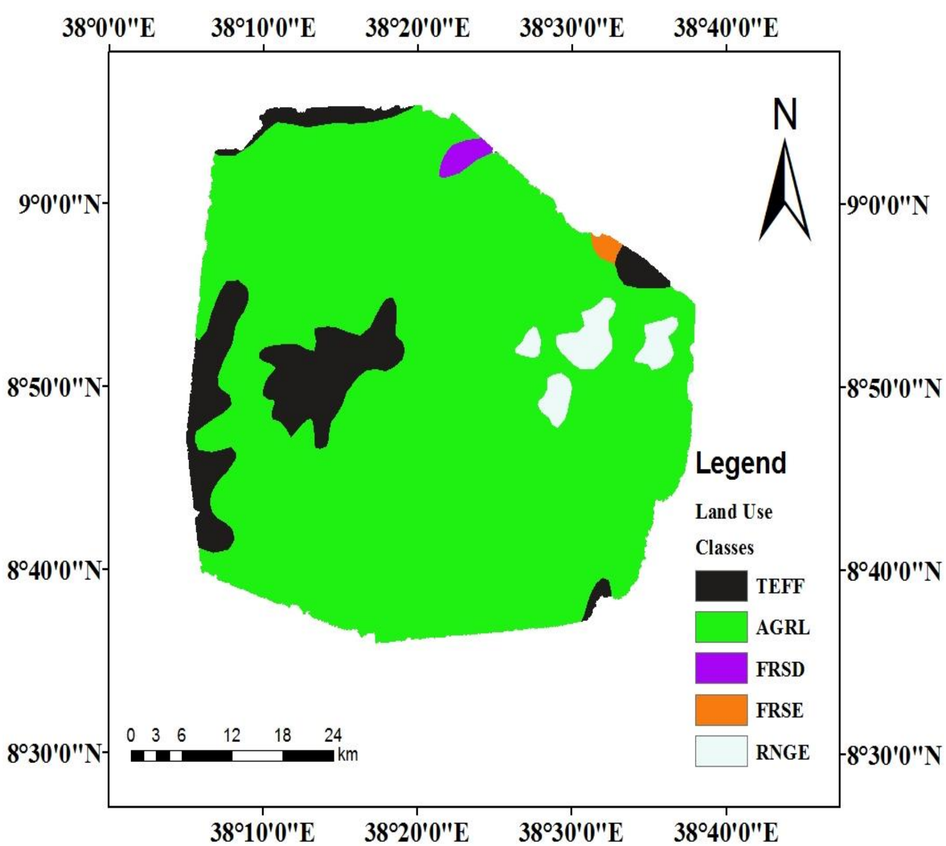

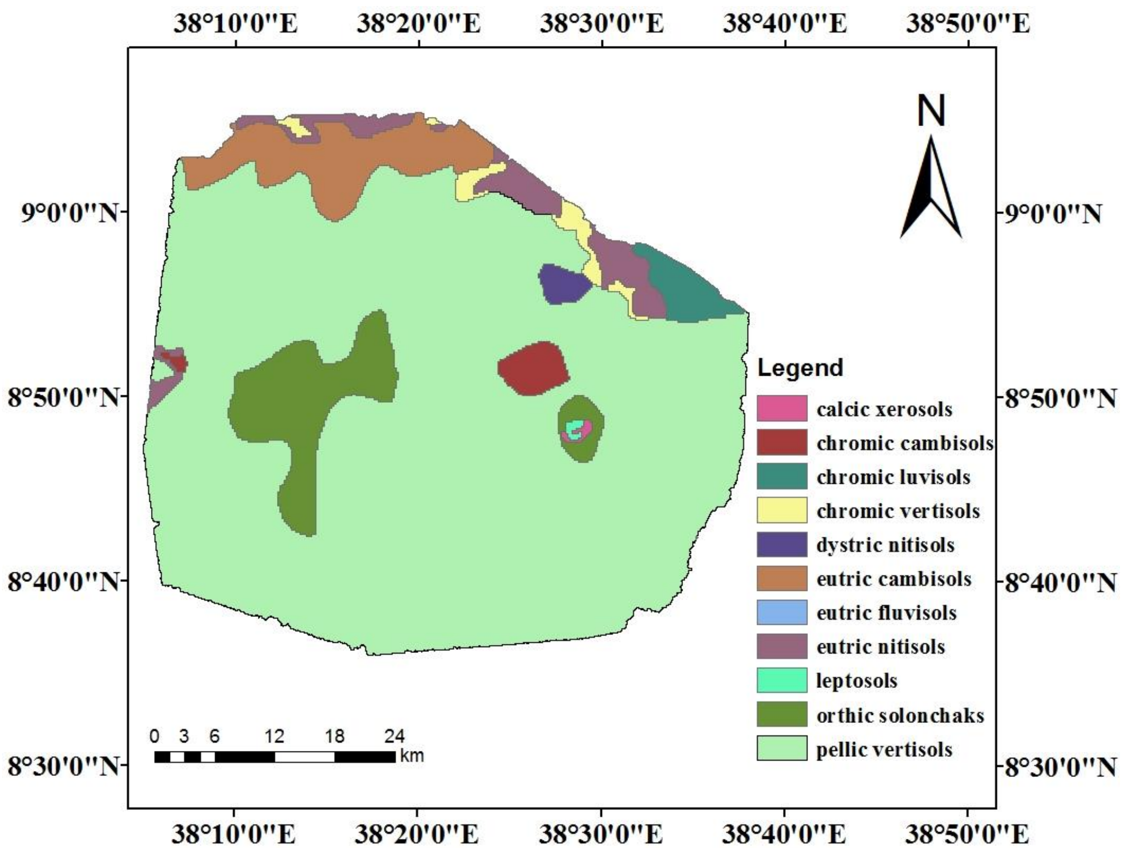

Appendex D: Value of a and b

Station	a	b
Addisalem	0.1237	1.925
Ginchi	0.31554	1.55373
Teji	0.12754	1.8979
Tefki	0.73635	1.0417
Tulubolo	0.46048	1.525